The Transit Method: Results from the Ground

- Results from individual transit search programs
- The Mass-Radius relationships (internal structure)
- Global Properties
- The Rossiter-McClaughlin Effect

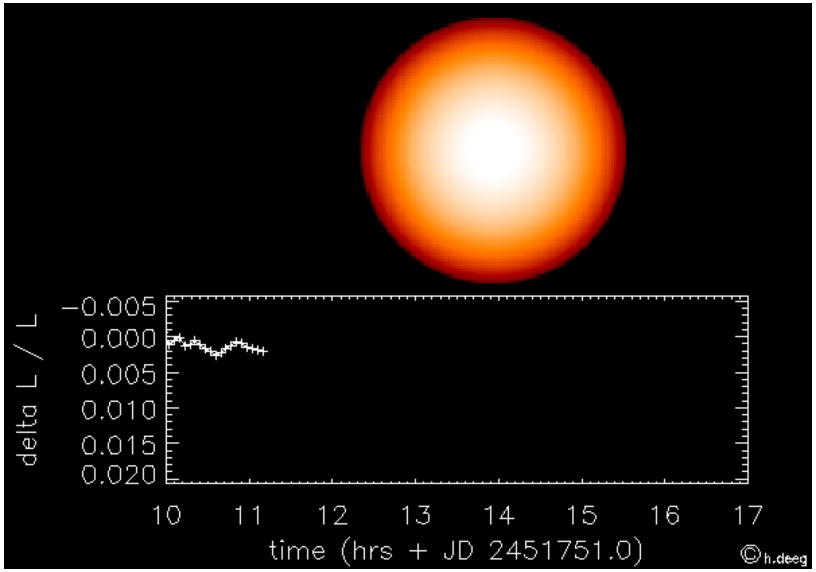

There are now 124 transiting extrasolar planets

First ones were detected by doing follow-up photometry of radial velocity planets. Now transit searches are discovering exoplanets

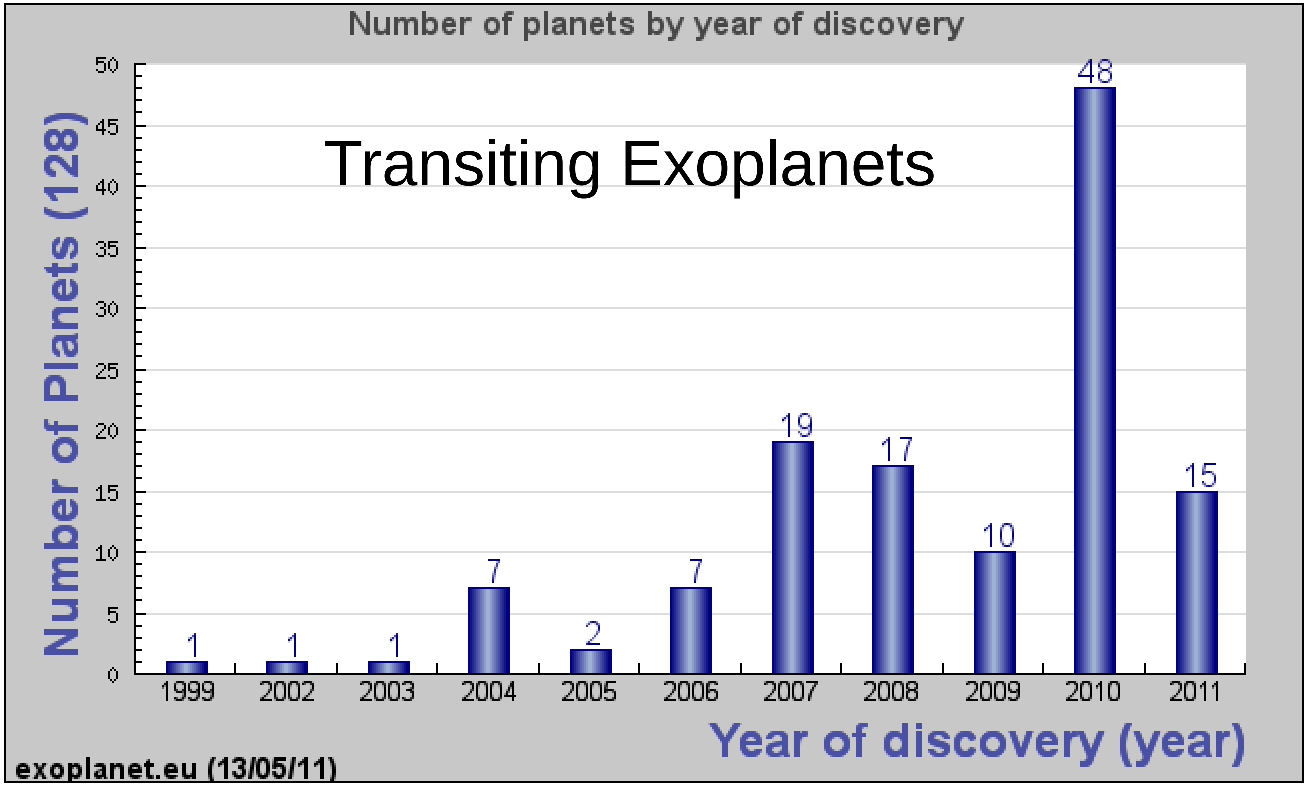

Radial Velocity Curve for HD 209458

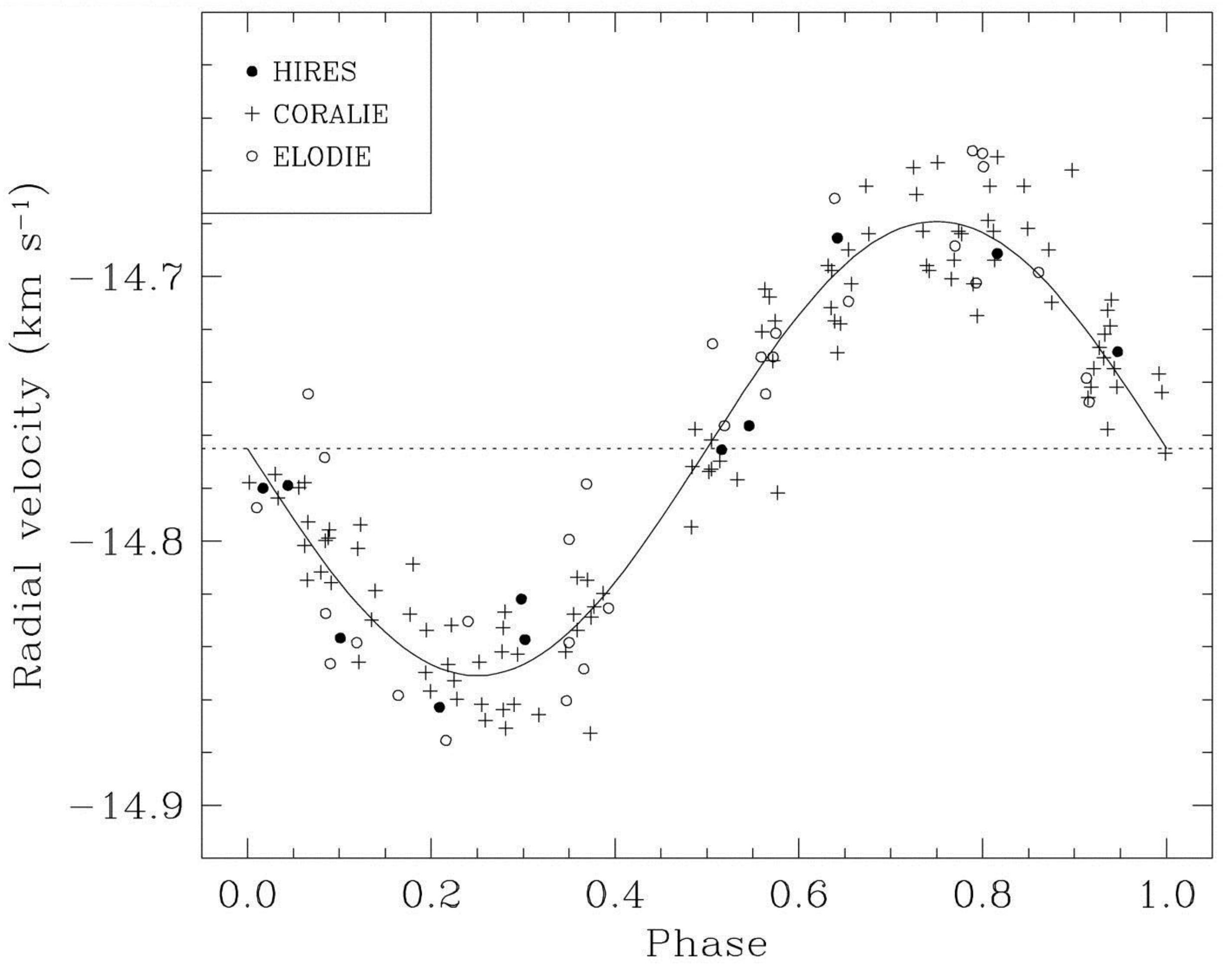

Period = 3.5 days

Msini = 0.63 M_{Jup}

The probability is 1 in 10 that a short period Jupiter will transit. HD 209458 was the 10th short period exoplanet searched for transits

Charbonneau et al. (2000): The observations that started it all:

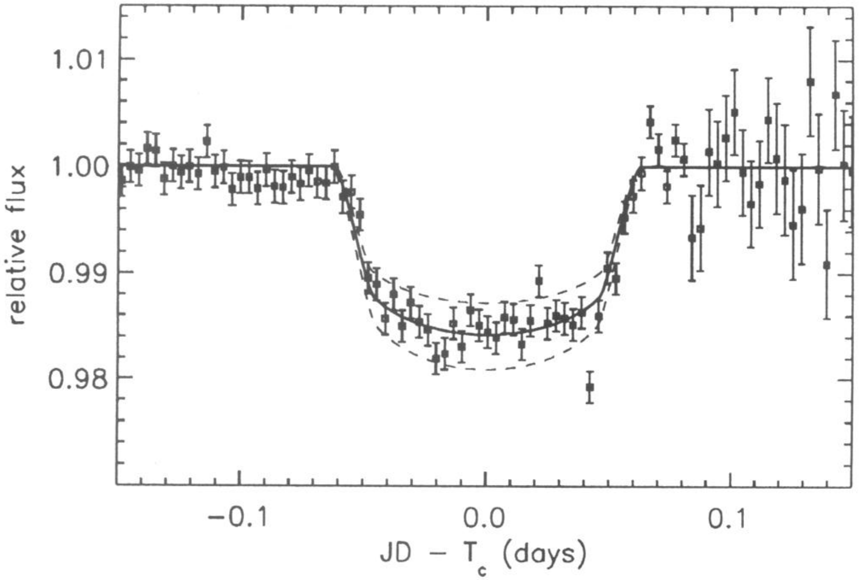

- Mass = 0.63 $M_{Jupiter}$
- Radius = 1.35 $R_{Jupiter}$
- Density = 0.38 g cm^{-3}

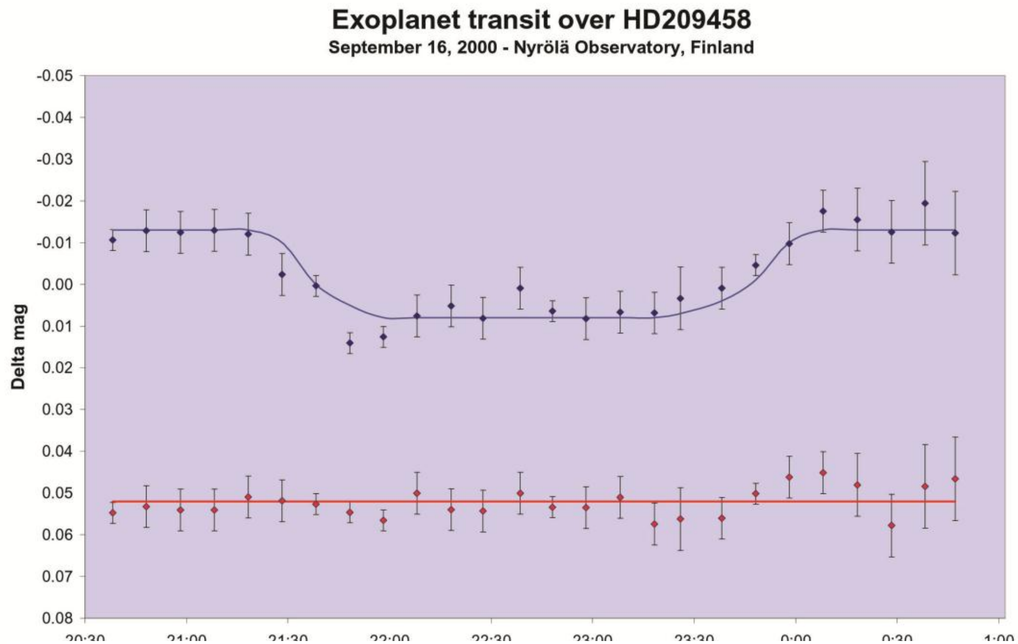

An amateur‘s light curve.

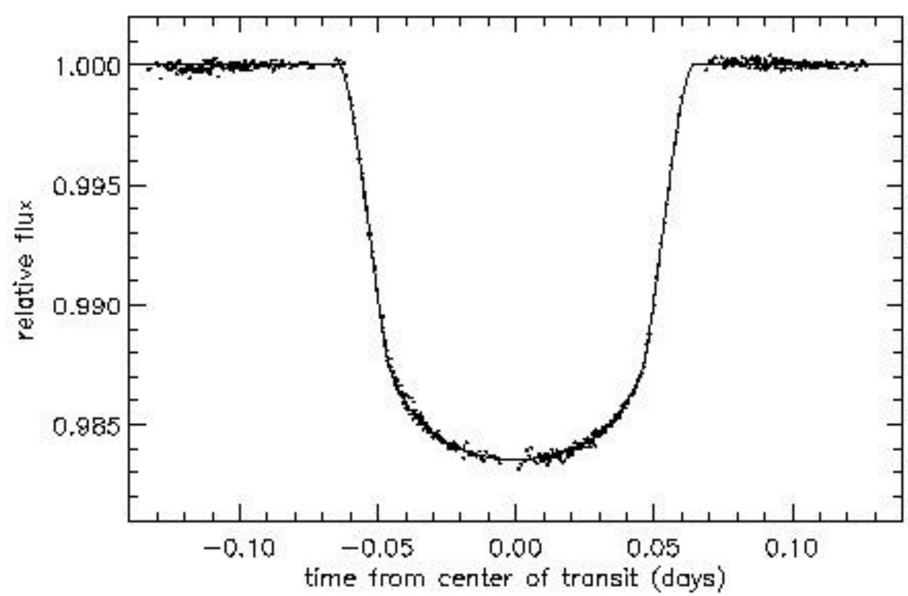

Hubble Space Telescope.

HD 209458b has a radius larger than expected.

Burrows et al. 2000

Evolution of the radius of HD 209458b and τ Boob

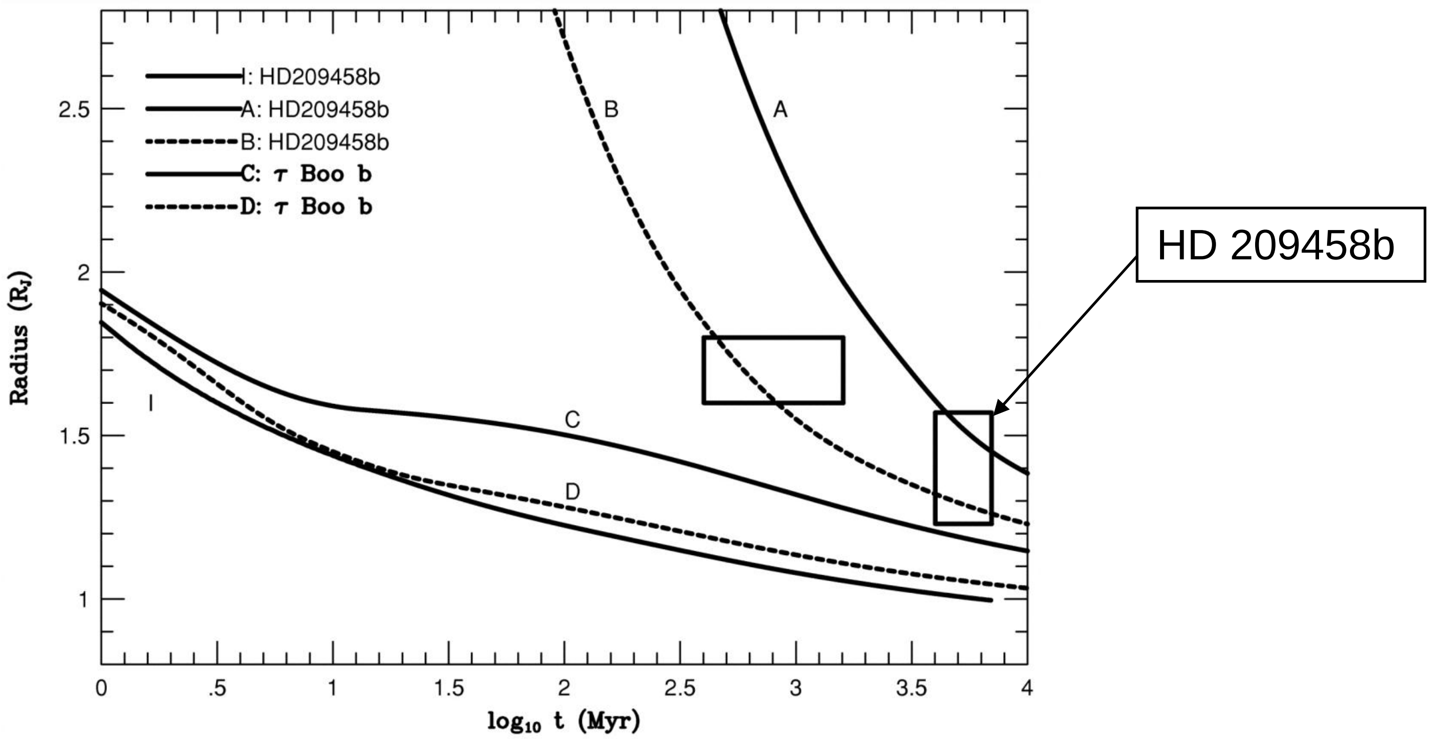

Models I, C, and D are for isolated planets

Models A and B are for irradiated planets.

One hypothesis for the large radius is that the stellar radiation hinders the contraction of the planet (it is hotter than it should be) so that it takes longer to contract. Another is tidal heating of the core of the planet if you have nonzero eccentricity

The OGLE Planets

- OGLE: Optical Gravitational Lens Experiment (http://www.astrouw.edu.pl/~ogle/)
    - 1.3m telescope looking into the galactic bulge
    - Mosaic of 8 CCDs: 35‘ x 35‘ field
    - Typical magnitude: V = 15-19
    - Designed for Gravitational Microlensing
    - **First planet discovered with the transit method**

The first planet found with the transit method

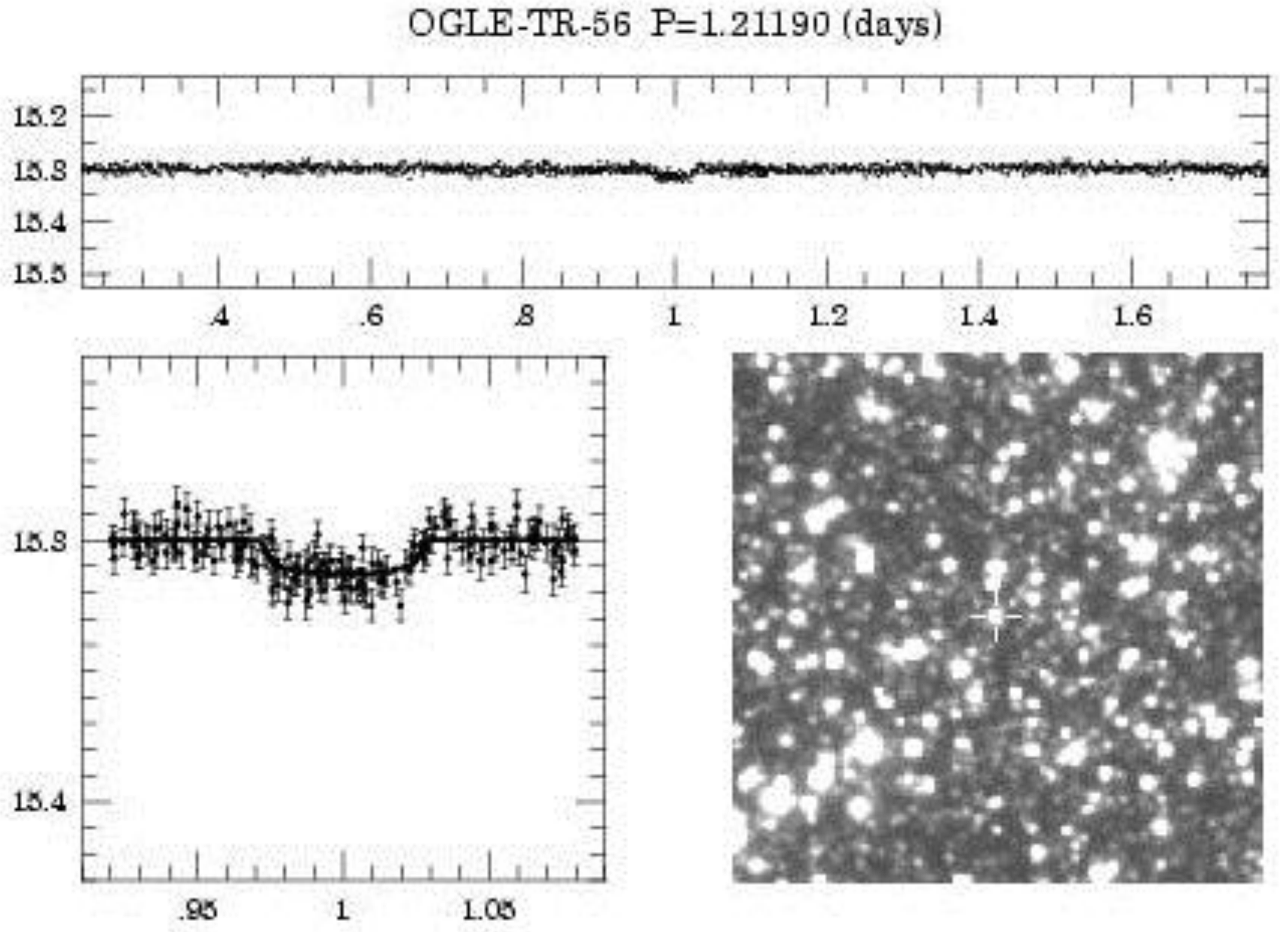

Konacki et al.

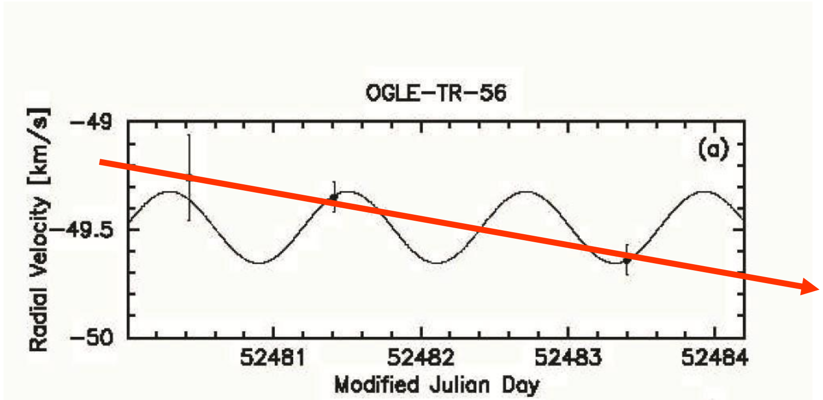

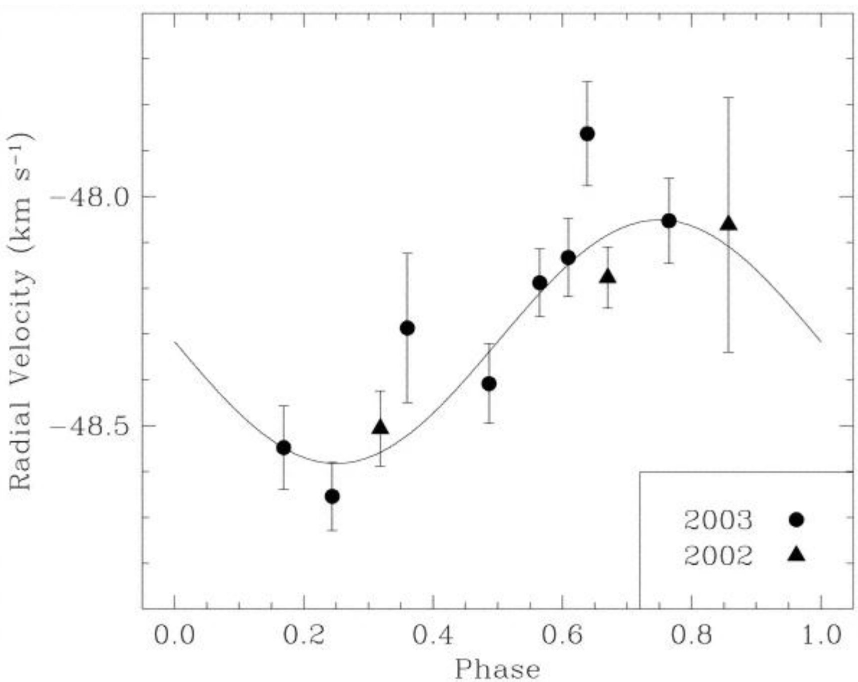

TABLE 2

PARAMETERS FOR OGLE-TR-56b

Parameter	Value
Orbital period (days)	1.2119189 ± 0.0000059
Transit epoch (HJD−2,400,000)	$52,075.1046 \pm 0.0017$
Center-of-mass velocity (km s^{-1})	-48.317 ± 0.045
Eccentricity (fixed)	0
Velocity semiamplitude (m s^{-1})	265 ± 38
Inclination angle (deg)	81.0 ± 2.2
Stellar mass ($M_\odot$) (adopted)	1.04 ± 0.05
Stellar radius ($R_\odot$) (adopted)	1.10 ± 0.10
Limb-darkening coefficient (I band)	0.56 ± 0.06
Planet mass (M_{Jup})	1.45 ± 0.23
Planet radius (R_{Jup})	1.23 ± 0.16
Planet density (g cm^{-3})	1.0 ± 0.3
Semimajor axis (AU)	0.0225 ± 0.0004

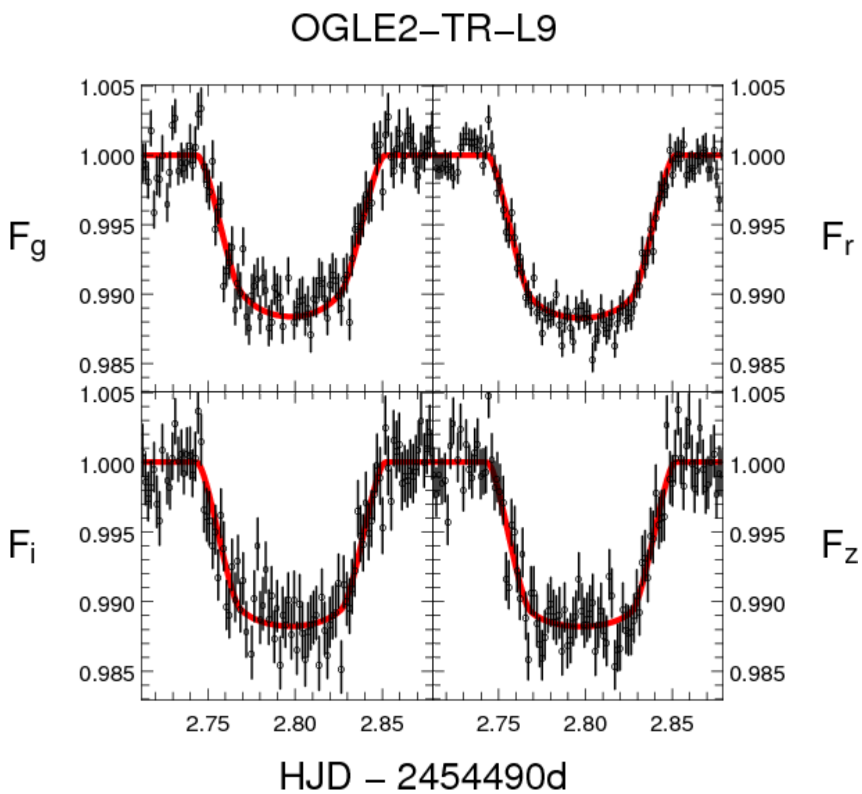

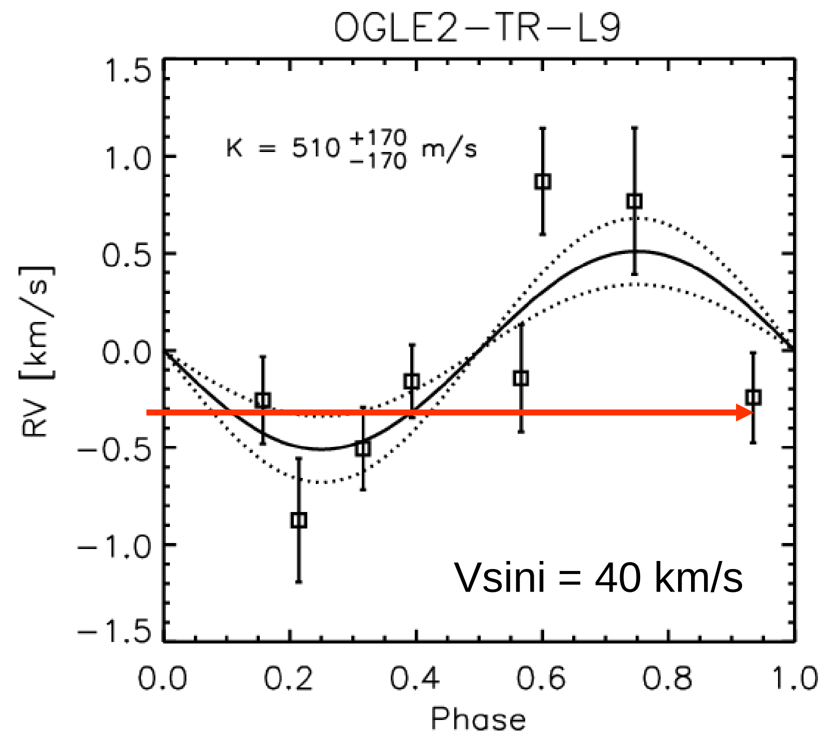

OGLE transiting planets: These produce low quality transits, they are faint, and they take up a large amount of 8m telescope time..

K = 510 ± 170 m/s

i= 79.8 ± 0.3

a= 0.0308

Mass = 4.5 M_J

Radius = 1.6 R_J

Spectral Type = F3 V

The OGLE Planets

Planet	Mass (M_{Jup})	Radius (R_{Jup})	Period (Days)	Year
OGLE2-TR-L9 b	4.5	1.6	2.48	2007
OGLE-TR-10 b	0.63	1.26	3.19	2004
OGLE-TR-56 b	1.29	1.3	1.21	2002
OGLE-TR-111 b	0.53	1.07	4.01	2004
OGLE-TR-113 b	1.32	1.09	1.43	2004
OGLE-TR-132 b	1.14	1.18	1.69	2004
OGLE-TR-182 b	1.01	1.13	3.98	2007
OGLE-TR-211 b	1.03	1.36	3.68	2007

Prior to OGLE all the RV planet detections had periods greater than about 3 days.

The last OGLE planet was discovered in 2007. Most likely these will be the last because the target stars are too faint.

The TrES Planets

- TrES: Trans-atlantic Exoplanet Survey (STARE is a member of the network http://www.hao.ucar.edu/public/research/stare/)
  - Three 10cm telescopes located at Lowell Observtory, Mount Palomar and the Canary Islands
  - 6.9 square degrees
  - 4 Planets discovered

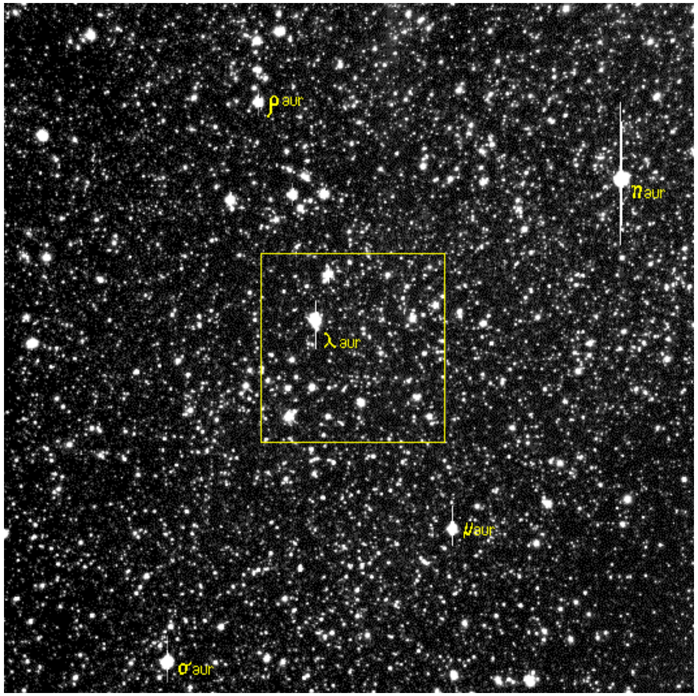

TrEs 2b

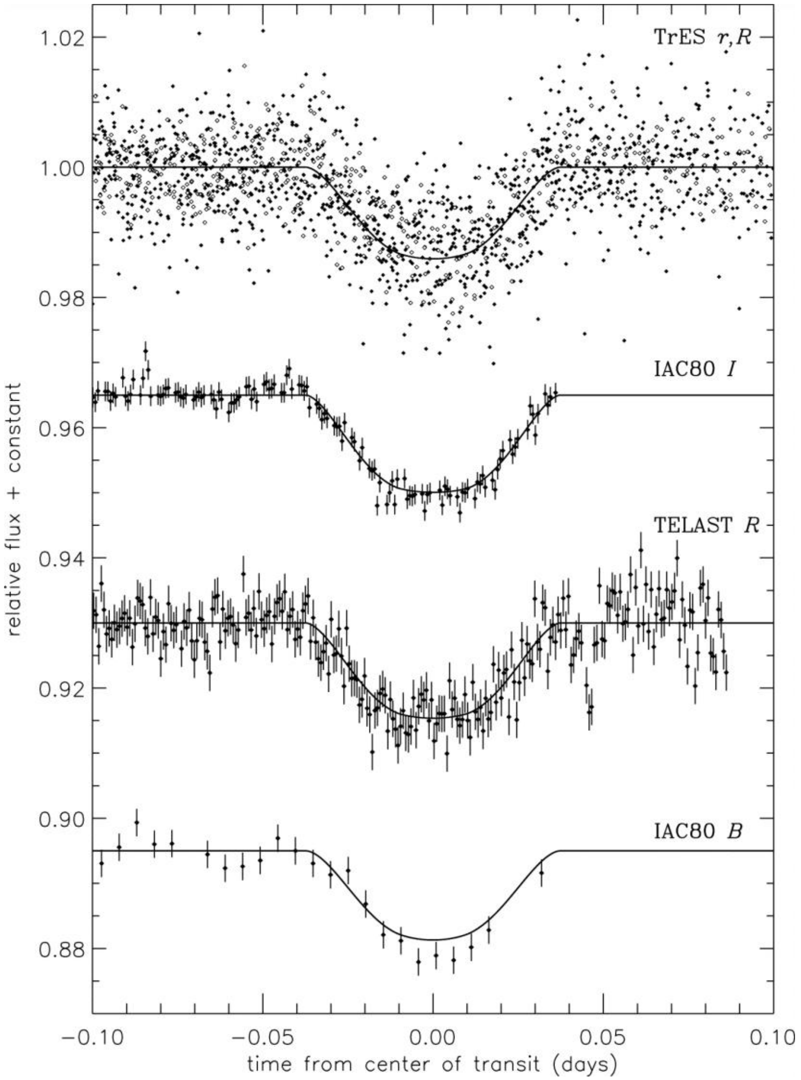

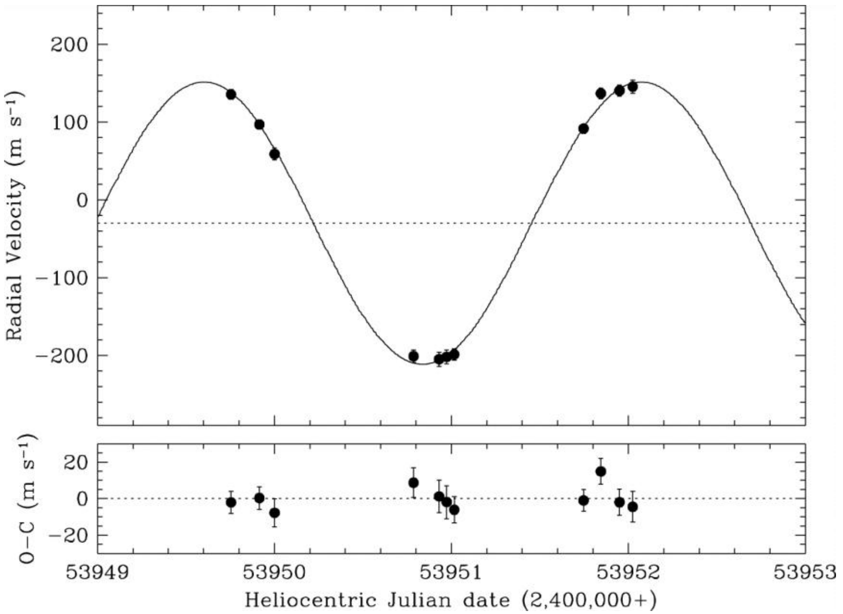

P = 2.47 d

M = 1.28 $M_{Jupiter}$

R = 1.24 $R_{Jupiter}$

i = 83.9 deg

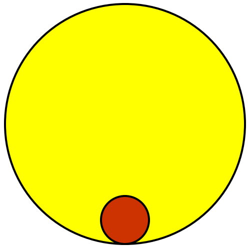

The HAT Planets

• HATNet: Hungarian-made Automated Telescope (http://www.cfa.harvard.edu/~gbakos/HAT/

- Six 11cm telescopes located at two sites: Arizona and Hawaii
- 8 x 8 square degrees
- > 20 Planets discovered

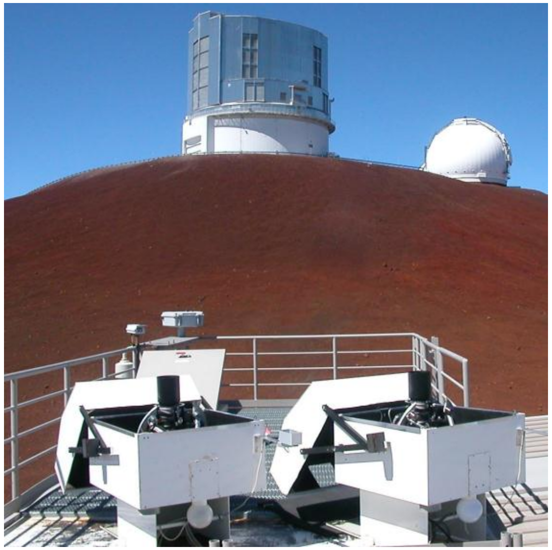

HAT-P-12b

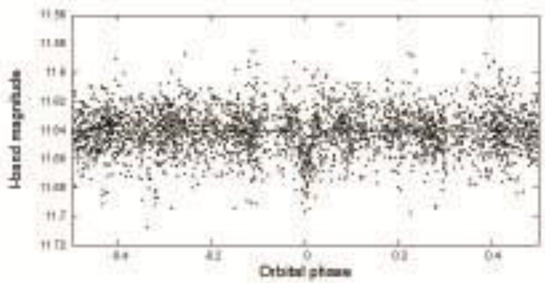

FIG. 1.— The unbinned light curve of HAT-P-12 including all 2927 instrumental I band 5.5-min cadence measurements obtained with the HAT-5 (Arizona) telescope of HATNet (see text for details), and folded with the period of $P = 3.2130598$ days (which is the result of the fit described in § 3).

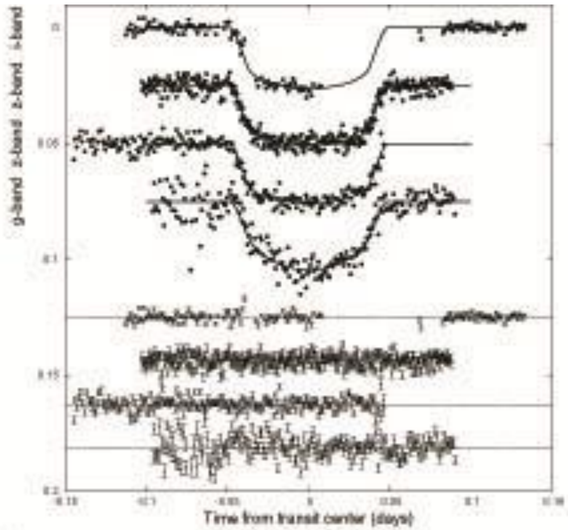

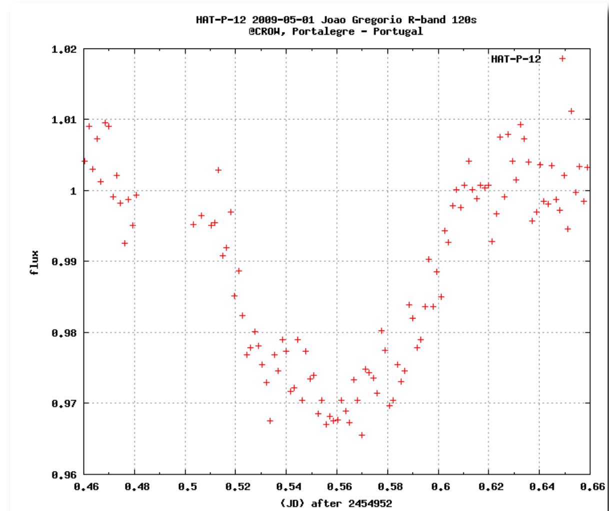

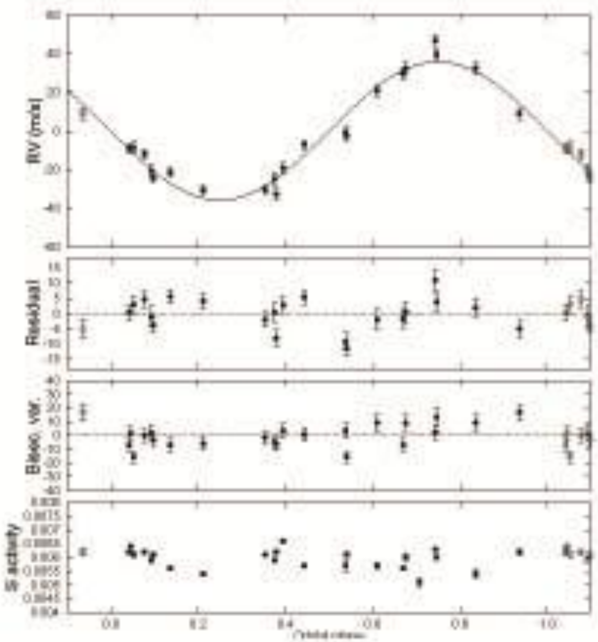

Star = K4 V

Planet Period = 3.2 days

Planet Radius = 0.96 R_{Jup}

Planet Mass = 0.21 M_{Jup} (~M_{Sat})

ρ = 0.3 g cm^{-3}

The best fitting model for HAT-P-12b has a core mass ≤ 10 M_{earth} and is still dominated by H/He (i.e. like Saturn and Jupiter and not like Uranus and Neptune). It is the lowest mass H/He dominated gas giant planet.

The WASP Planets

WASP: Wide Angle Search for Planets (http://www.superwasp.org). Also known as SuperWASP

- Array of 8 Wide Field Cameras
- Field of View: 7.8º x 7.8º
- 13.7 arcseconds/pixel
- Typical magnitude: V = 9-13
- >50 transiting planets discovered so far

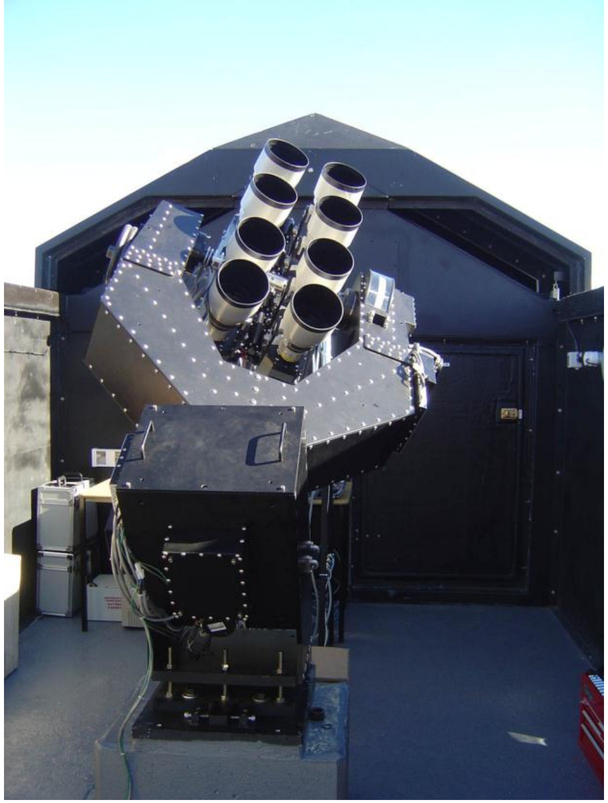

The First WASP Planet

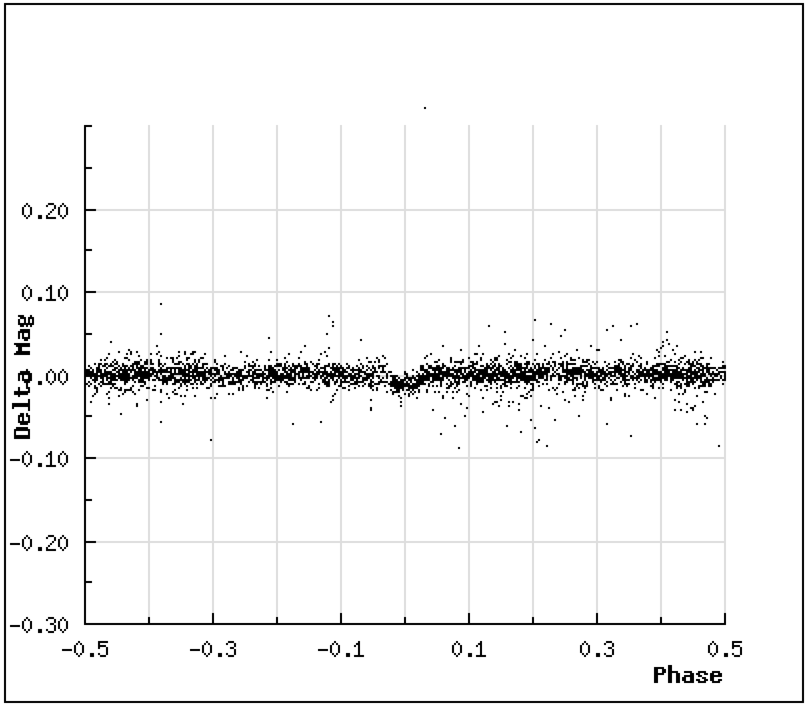

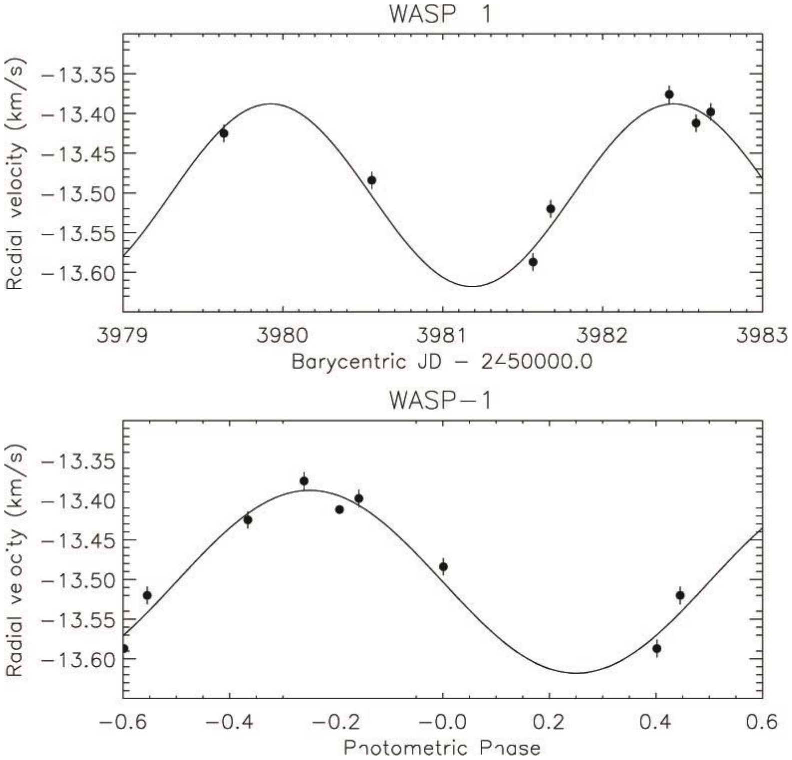

Coordinates	RA 00:20:40.07 Dec +31:59:23.7
Constellation	Pegasus
Apparent Visual Magnitude	11.79
Distance from Earth	1234 Light Years
WASP-1 Spectral Type	F7V
WASP-1 Photospheric Temperature	6200 K
WASP-1b Radius	1.39 Jupiter Radii
WASP-1b Mass	0.85 Jupiter Masses
Orbital Distance	0.0378 AU
Orbital Period	2.52 Days
Atmospheric Temperature	1800 K
Mid-point of Transit	2453151.4860 HJD

WASP 12: Hottest Transiting Giant Planet

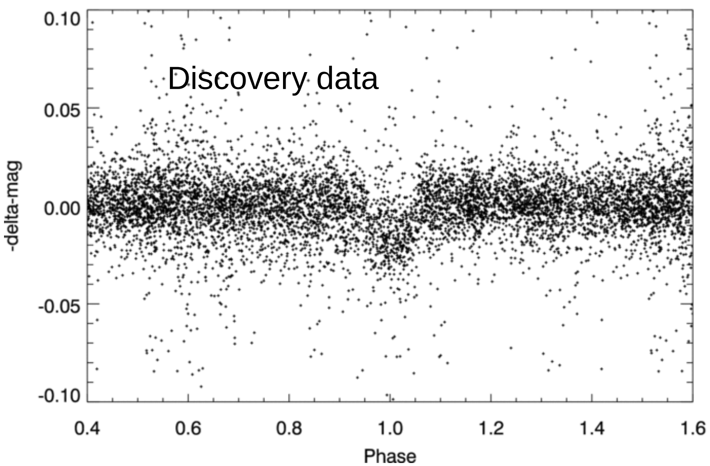

High quality light curve for accurate parameters

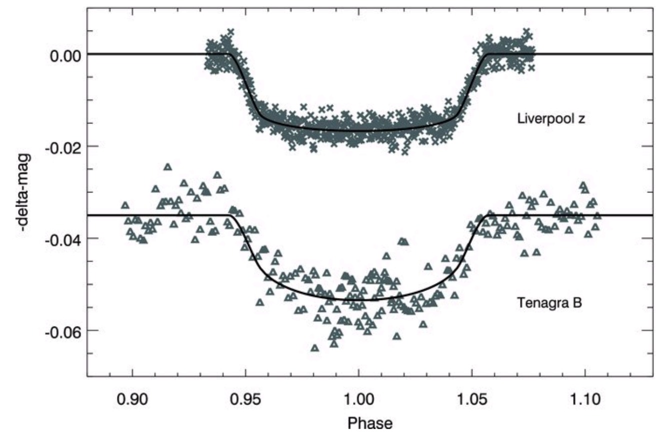

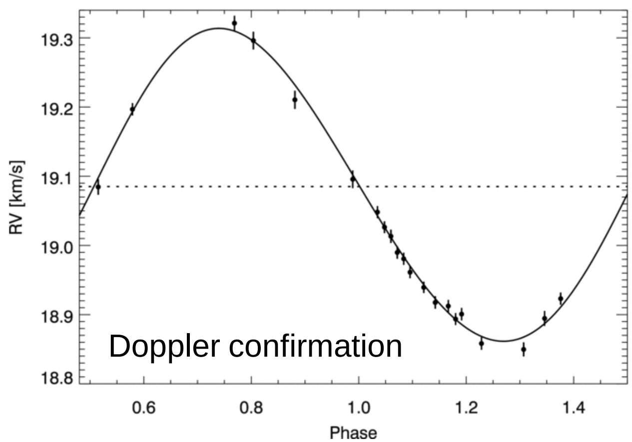

Orbital Period: 1.09 d

Transit duration: 2.6 hrs

Planet Mass: 1.41 $M_{Jupiter}$

Planet Radius: 1.79 $R_{Jupiter}$

Planet Temperature: 2516 K

Spectral Type of Host Star: F7 V

Comparison of WASP 12 to an M8 Main Sequence Star

Planet	M8 Star
Planet Mass: 1.41 $M_{Jupiter}$	Mass: 60 $M_{Jupiter}$
Planet Radius: 1.79 $R_{Jupiter}$	Radius: ~1 $R_{Jupiter}$
Planet Temperature: 2516 K	Teff: ~ 2800 K

WASP 12 has a smaller mass, larger radius, and comparable effective temperature than an M8 dwarf. Its atmosphere should look like an M9 dwarf or L0 brown dwarf. One difference: above temperature for the planet is only on the day side because the planet does not generate its own energy

GJ 436: The First Transiting Neptune

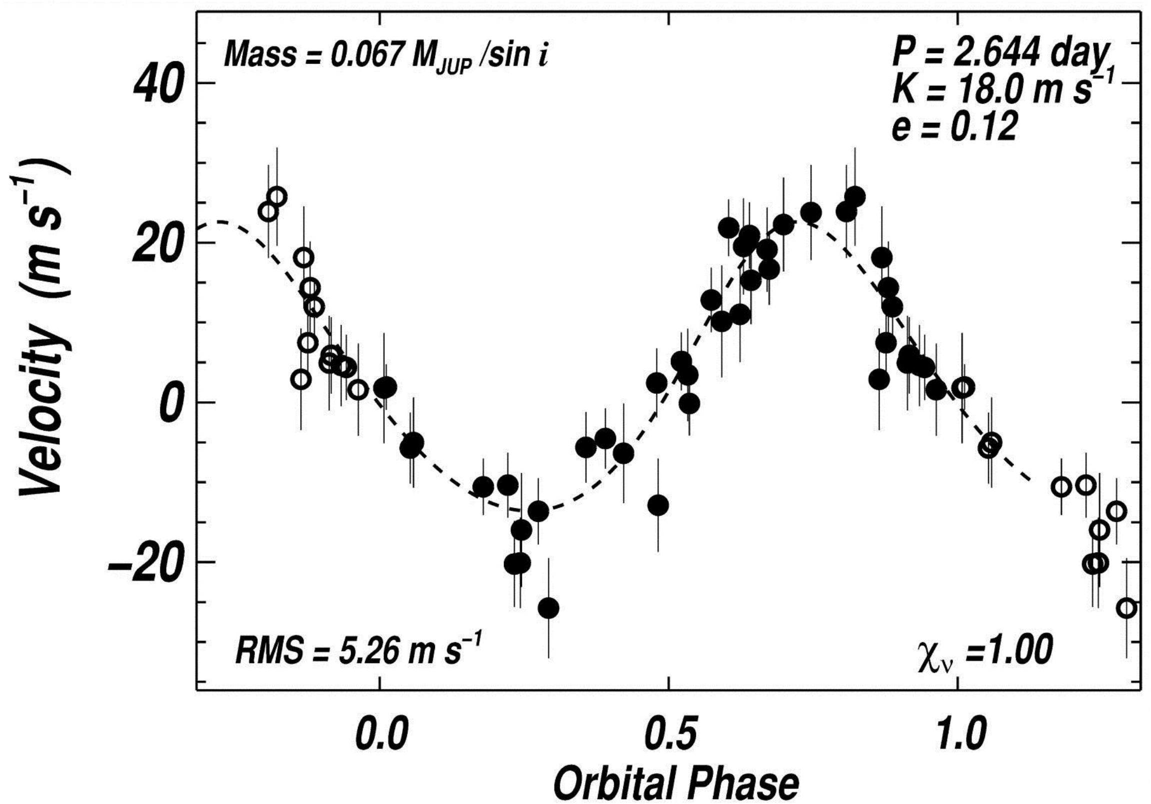

Host Star:

Butler et al. 2004

Mass = 0.4 $M_{\odot}$ (M2.5 V)

Special Transits: GJ 436

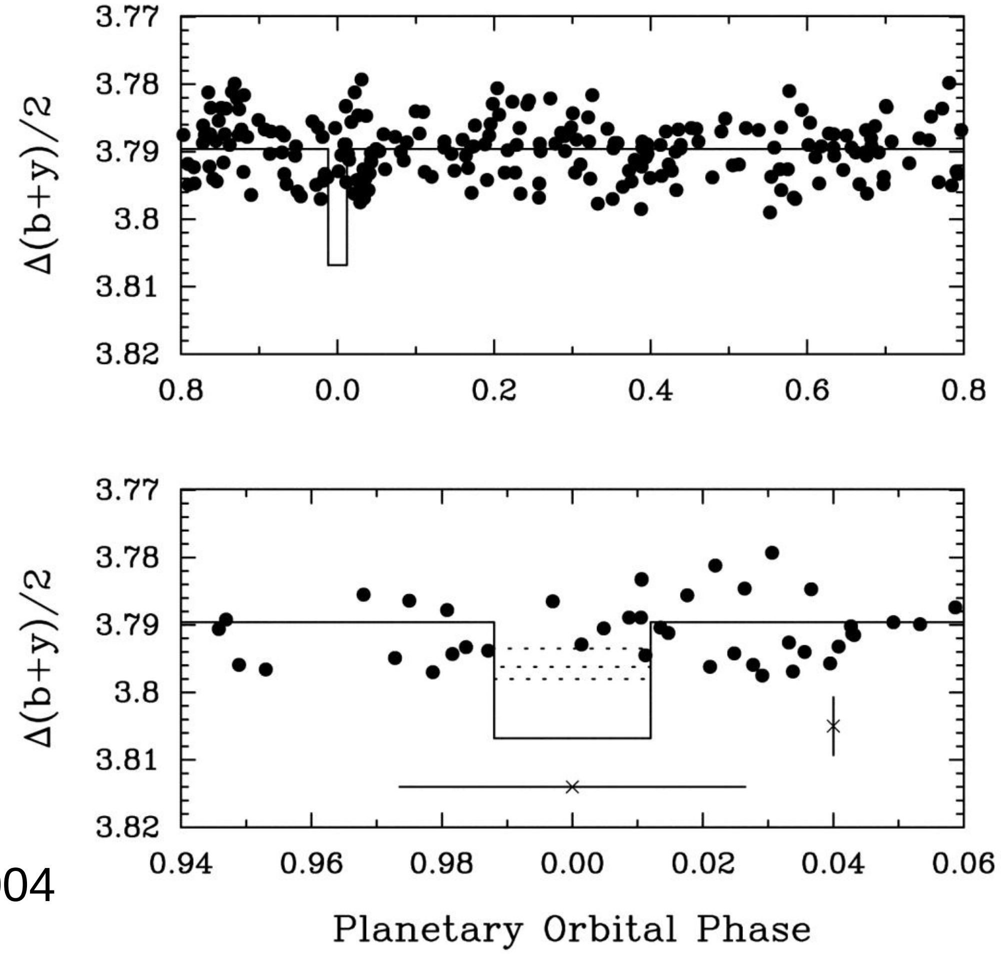

Butler et al. 2004

„Photometric transits of the planet across the star are ruled out for gas giant compositions and are also unlikely for solid compositions“

The First Transiting Hot Neptune!

Gillon et al. 2007

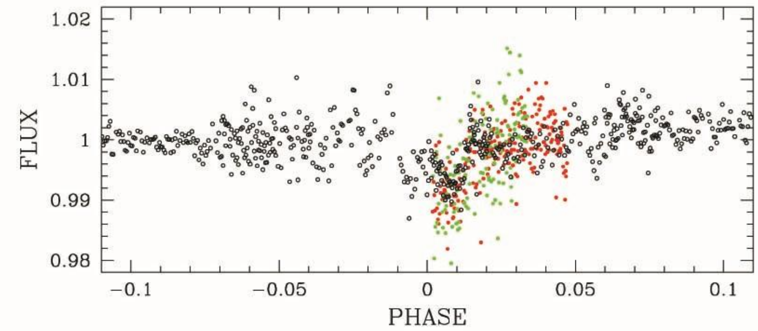

Fig. 1. OFXB (*black*) and Wise (*red: 1m, green: 46cm*) photometry phase-folded using the ephemerids and period presented in Maness et al. (2007).

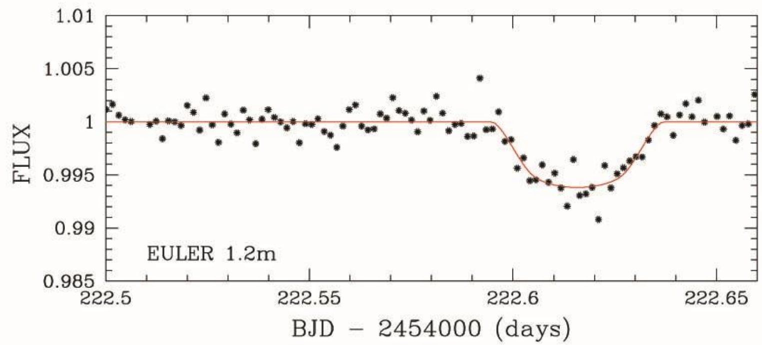

Fig. 2. Euler V-band transit photometry. The best-fit transit curve is superimposed in red.

GJ 436

Star	
Stellar mass [$M_\odot$]	0.44 (± 0.04)
Planet	
Period [days]	2.64385 ± 0.00009
Eccentricity	0.16 ± 0.02
Orbital inclination	86.5 ± 0.2
Planet mass [M_E]	22.6 ± 1.9
Planet radius [R_E]	$3.95^{+0.41}_{-0.28}$

Mean density = 1.95 gm cm^{-3}, slightly higher than Neptune (1.64)

HD 17156: An eccentric orbit planet

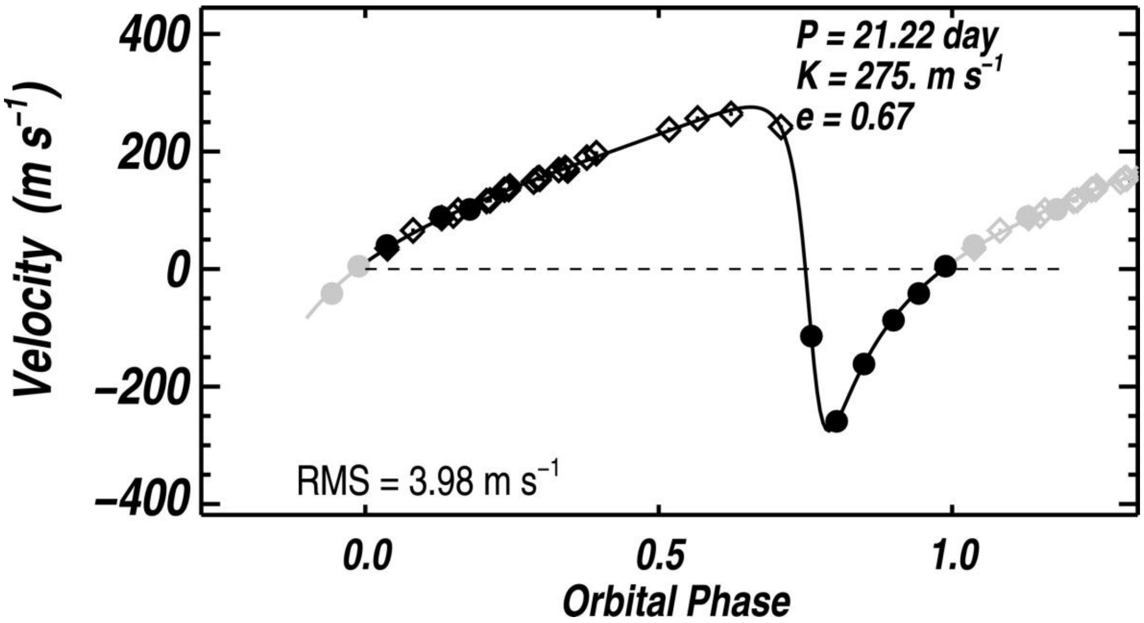

$M = 3.11\ M_{Jup}$

Probability of a transit ~ 3%

Barbieri et al. 2007

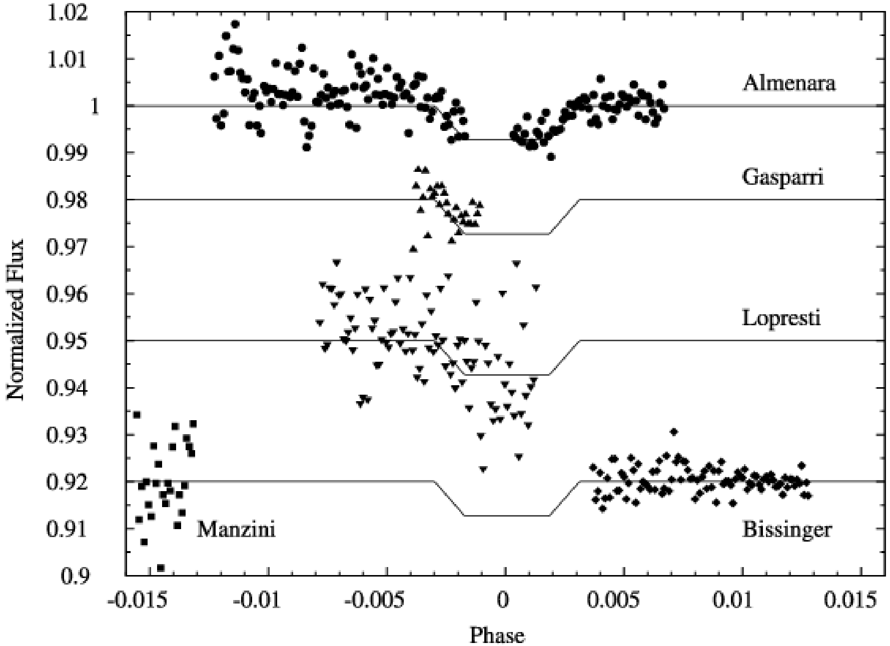

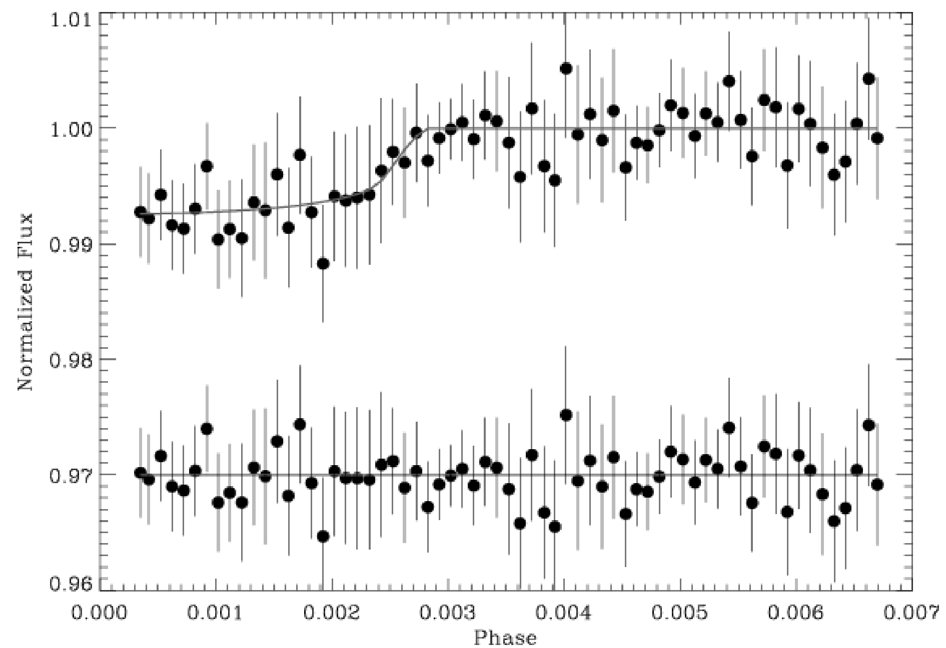

$R = 0.96\ R_{Jup}$

Mean density = 4.88 g/cm^3

Mean for M2 star $\approx$ 4.3 g/cm^3

HD 80606: Long period and eccentric

R = 1.03 R_{Jup} ρ = 4.44 (cgs)

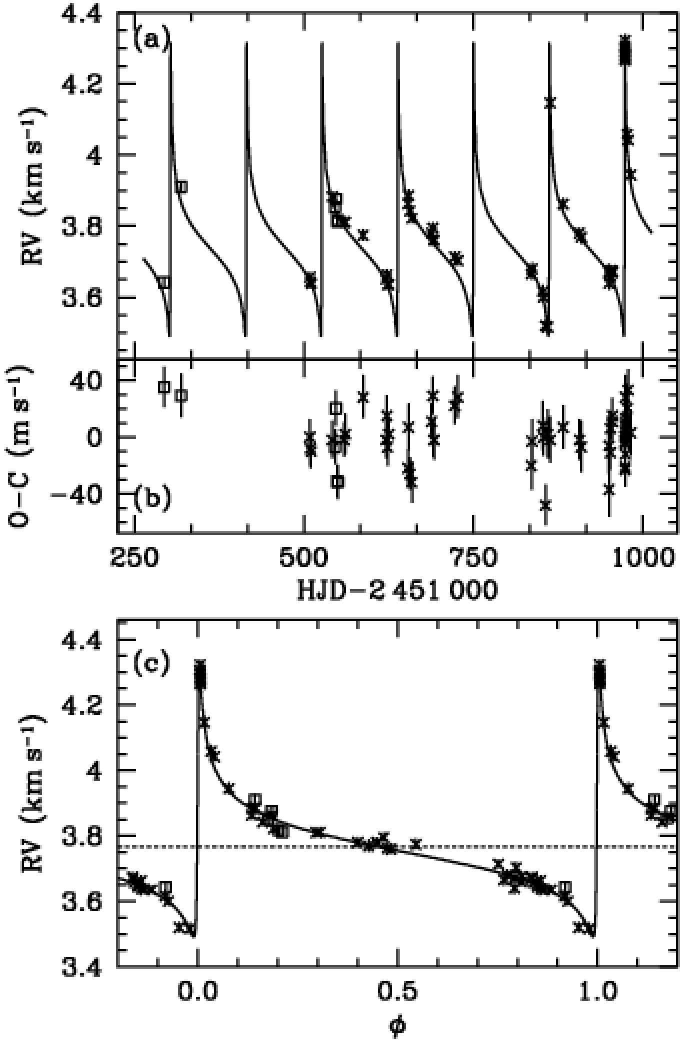

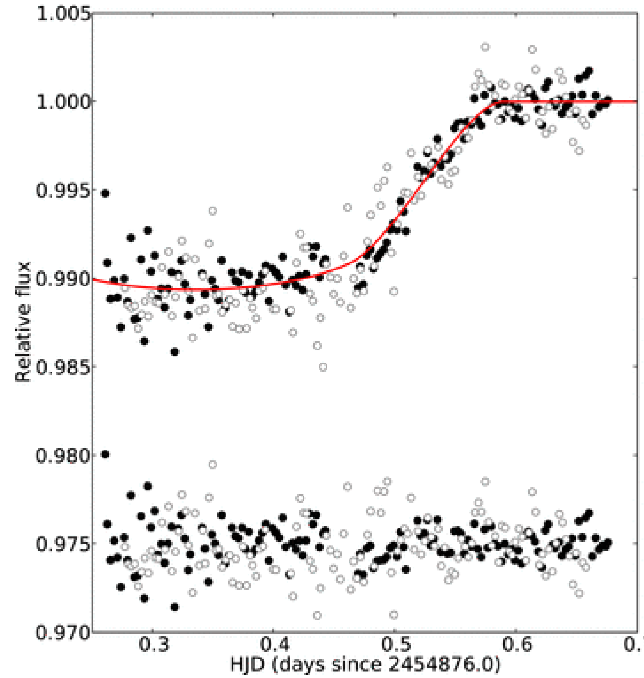

P	days	111.81 ± 0.23
T	HJD	2 451 973.72 ± 0.29
e		0.927 ± 0.012
γ	$\mathrm{km\,s^{-1}}$	3.767 ± 0.010
w	°	291.0 ± 6.7
K_1	$\mathrm{m\,s^{-1}}$	411 ± 31
$\Delta RV_{\mathrm{H-E}}$	$\mathrm{m\,s^{-1}}$	1.5 ± 8.5
$a_1 \sin i$	10^{-3} AU	1.581 ± 0.037
$f_1(m)$	$10^{-8}\ M_\odot$	4.26 ± 0.29
$m_2 \sin i$	M_{Jup}	3.90 ± 0.09
N		55(E) + 6(H)
$\sigma_{\mathrm{O-C}}$	$\mathrm{m\,s^{-1}}$	17.7 (E:16.3, H:29.9)

a = 0.45 AU

d_{min} = 0.03 AU d_{max} = 0.87 AU

MEarth-1b: A transiting Superearth

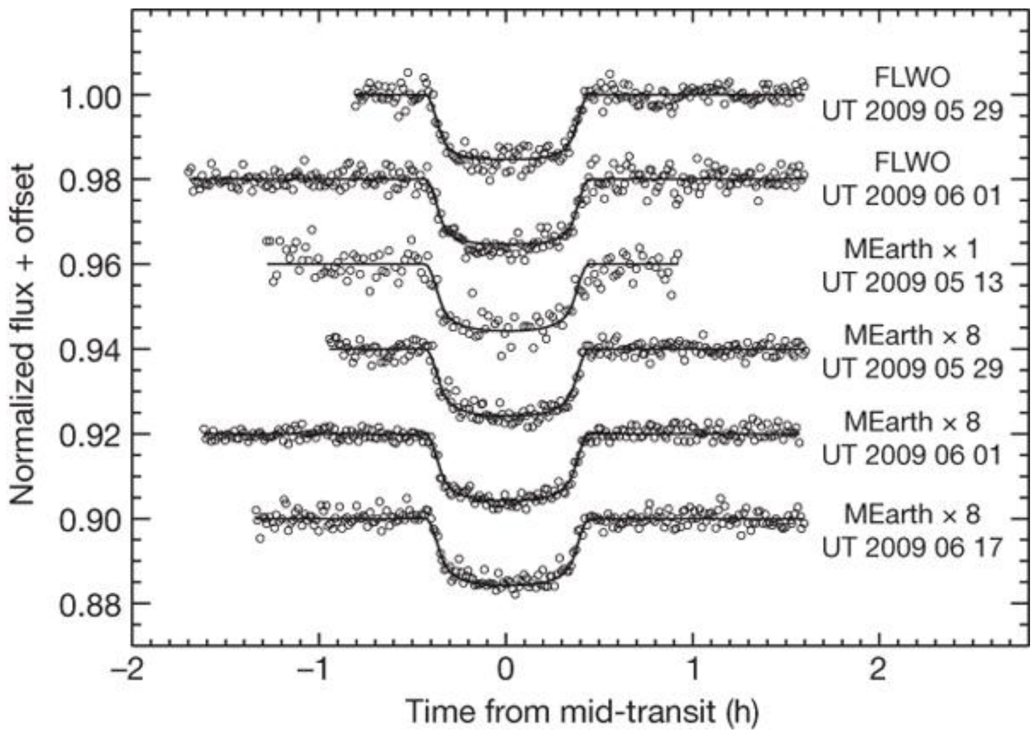

D Charbonneau *et al. Nature* **462**, 891-894 (2009) doi:10.1038/nature08679

nature

Change in radial velocity of GJ1214.

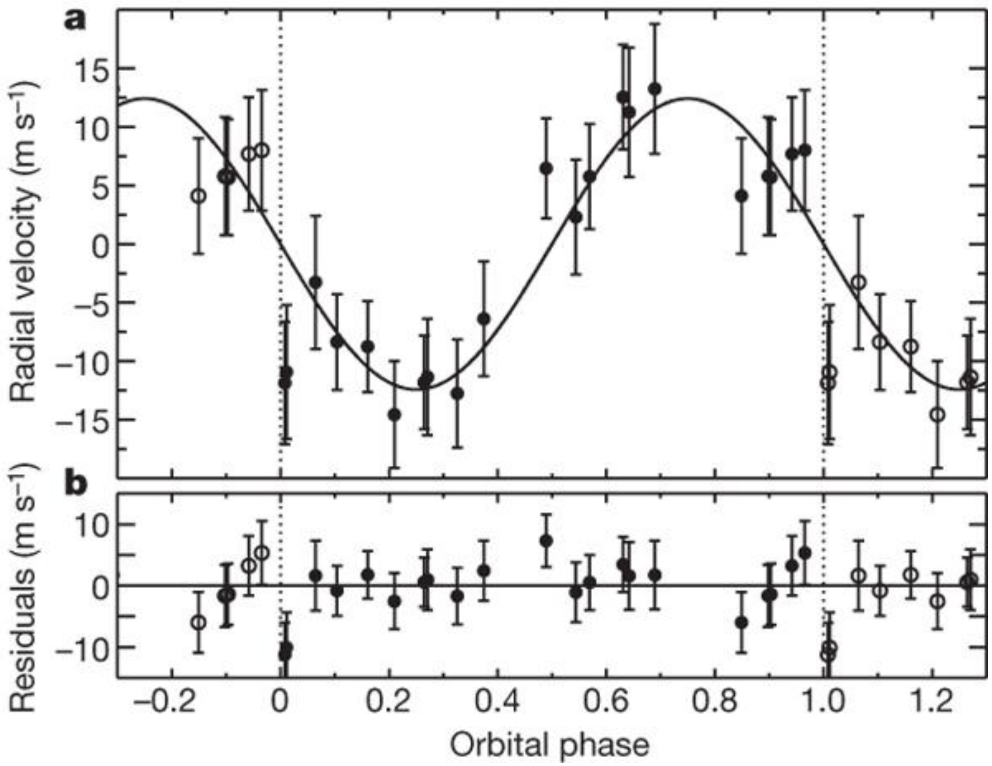

D Charbonneau *et al. Nature* **462**, 891-894 (2009) doi:10.1038/nature08679

nature

Table 1 | System parameters for GJ 1214

Parameter	Value
Orbital period, P (days)	1.5803925 ± 0.0000117
Times of centre of transit, T_c (HJD)	$2454964.944208 \pm 0.000403$
	$2454980.7479702 \pm 0.0000903$
	$2454983.9087558 \pm 0.0000901$
	$2454999.712703 \pm 0.000126$
Planet/star radius ratio, R_p/R_s	0.1162 ± 0.00067
Scaled semimajor axis, a/R_s	14.66 ± 0.41
Impact parameter, b	$0.354^{+0.061}_{-0.082}$
Orbital inclination, i (deg)	$88.62^{+0.35}_{-0.28}$
Radial velocity semi-amplitude, K (m s^{-1})	12.2 ± 1.6
Systemic velocity, γ (m s^{-1})	$-21,100 \pm 1,000$
Orbital eccentricity, e	<0.27 (95% confidence)
Stellar mass, M_s	$0.157 \pm 0.019 M_\odot$
Stellar radius, R_s	$0.2110 \pm 0.0097 R_\odot$
Stellar density, ρ_s (kg m^{-3})	$23,900 \pm 2,100$
Log of stellar surface gravity (CGS units), log g_s	4.991 ± 0.029
Stellar projected rotational velocity, $v \sin i$ (km s^{-1})	<2.0
Stellar parallax (mas)	77.2 ± 5.4
Stellar photometry	
V	15.1 ± 0.6
I	11.52 ± 0.1
J	9.750 ± 0.024
H	9.094 ± 0.024
K	8.782 ± 0.020
Stellar luminosity, L_s	$0.00328 \pm 0.00045 L_\odot$
Stellar effective temperature, T_{eff} (K)	$3,026 \pm 130$
Planetary radius, R_p	$2.678 \pm 0.13 R_\oplus$
Planetary mass, M_p	$6.55 \pm 0.98 M_\oplus$
Planetary density, ρ_p (kg m^{-3})	1870 ± 400
Planetary surface acceleration under gravity, g_p (m s^{-2})	8.93 ± 1.3
Planetary equilibrium temperature, T_{eq} (K)	
Assuming a Bond albedo of 0	555
Assuming a Bond albedo of 0.75	393

To convert the photometric and radial velocity parameters into physical parameters for the system, we require a constraint on the stellar mass. Using the observed parallax distance[26] of 12.95 ± 0.9 pc and apparent K-band brightness, we employ an empirical relation[27] between stellar mass and absolute K-band magnitude to estimate the stellar mass. With this value we find the planetary radius and mass. The uncertainty on the planet mass is the quadrature sum of the propagated uncertainties on the radial-velocity amplitude and those from the uncertainty in the stellar mass, which contribute $0.85 M_\oplus$ and $0.50 M_\oplus$ to the error budget, respectively. We use the observed $I - K$ colour and an empirical relation[28] to estimate the bolometric correction and subsequently the stellar luminosity and stellar effective temperature (assuming the stellar radius quoted in the table). Using the luminosity, we estimate a planetary equilibrium temperature, assuming a value for the Bond albedo. HJD, heliocentric Julian date.

$\rho = 1.87$ (g/cm^3)

So what do all of these transiting planets tell us?

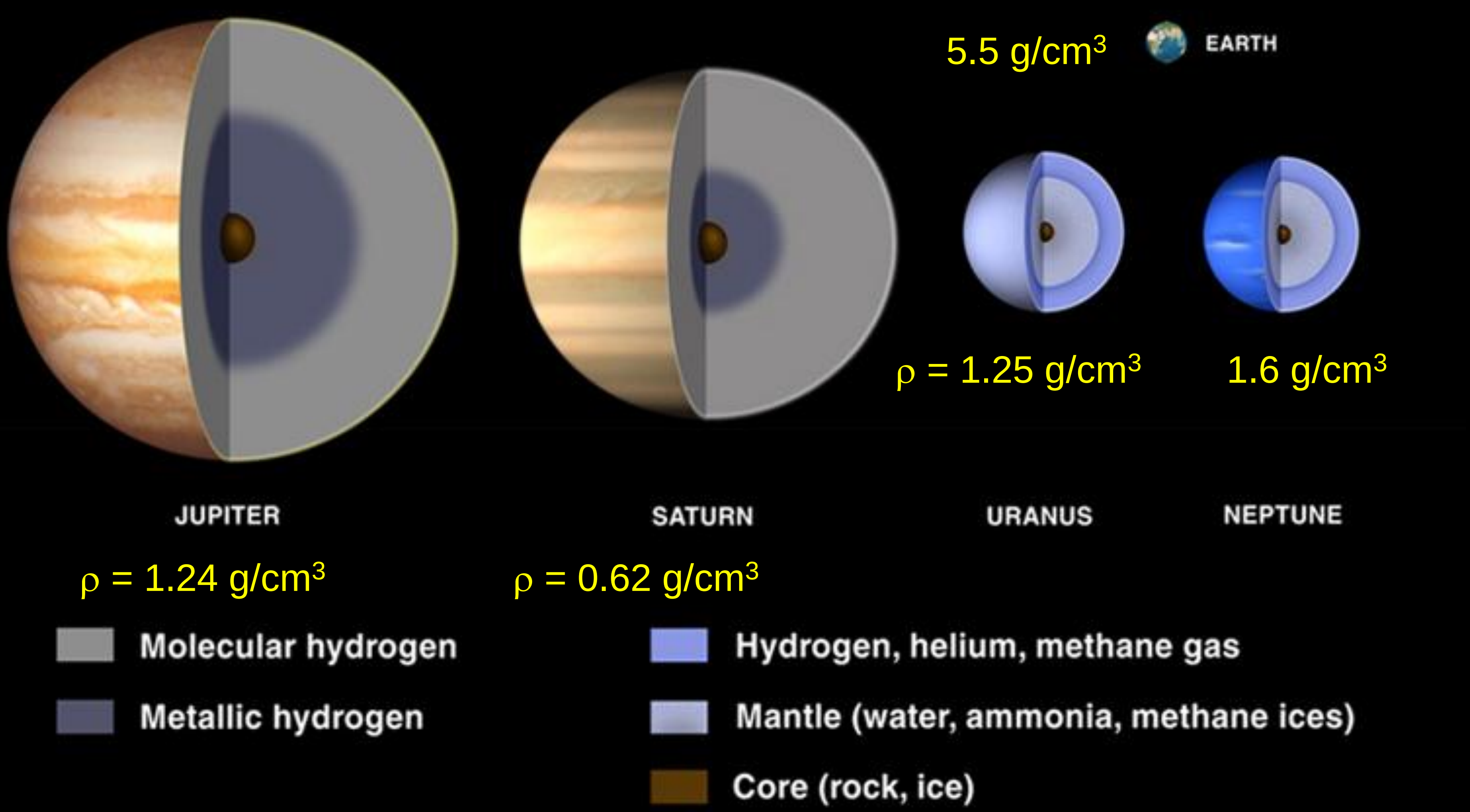

The density is the first indication of the internal structure of the exoplanet

Solar System Object	**ρ (g cm^{-3})**
Mercury	5.43
Venus	5.24
Earth	5.52
Mars	3.94
Jupiter	1.24
Saturn	0.62
Uranus	1.25
Neptune	1.64
Pluto	2
Moon	3.34
Carbonaceous Meteorites	2–3.5
Iron Meteorites	7–8
Comets	0.06-0.6

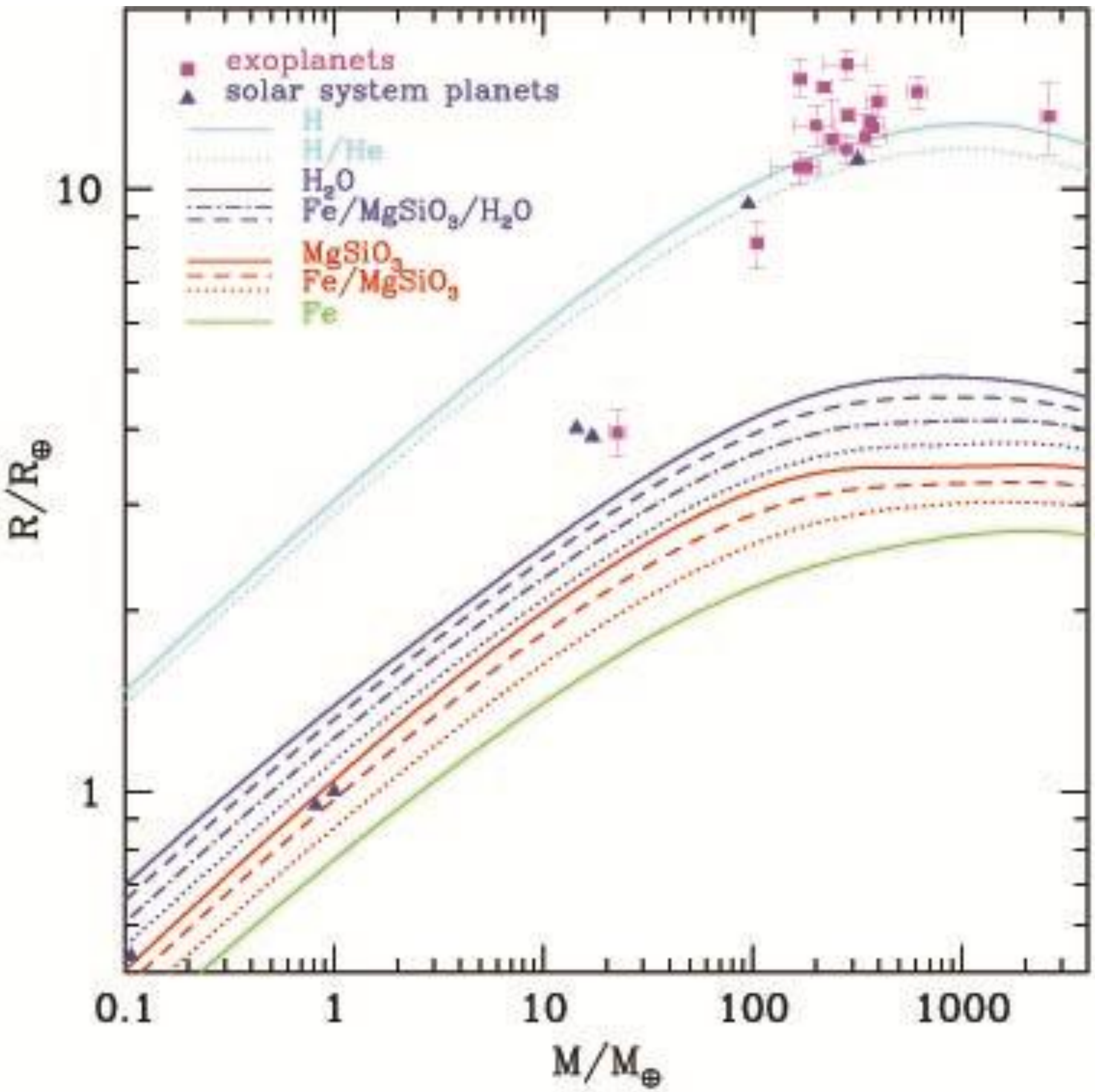

Take your favorite composition and calculate the mass-radius relationship

Masses and radii of transiting planets.

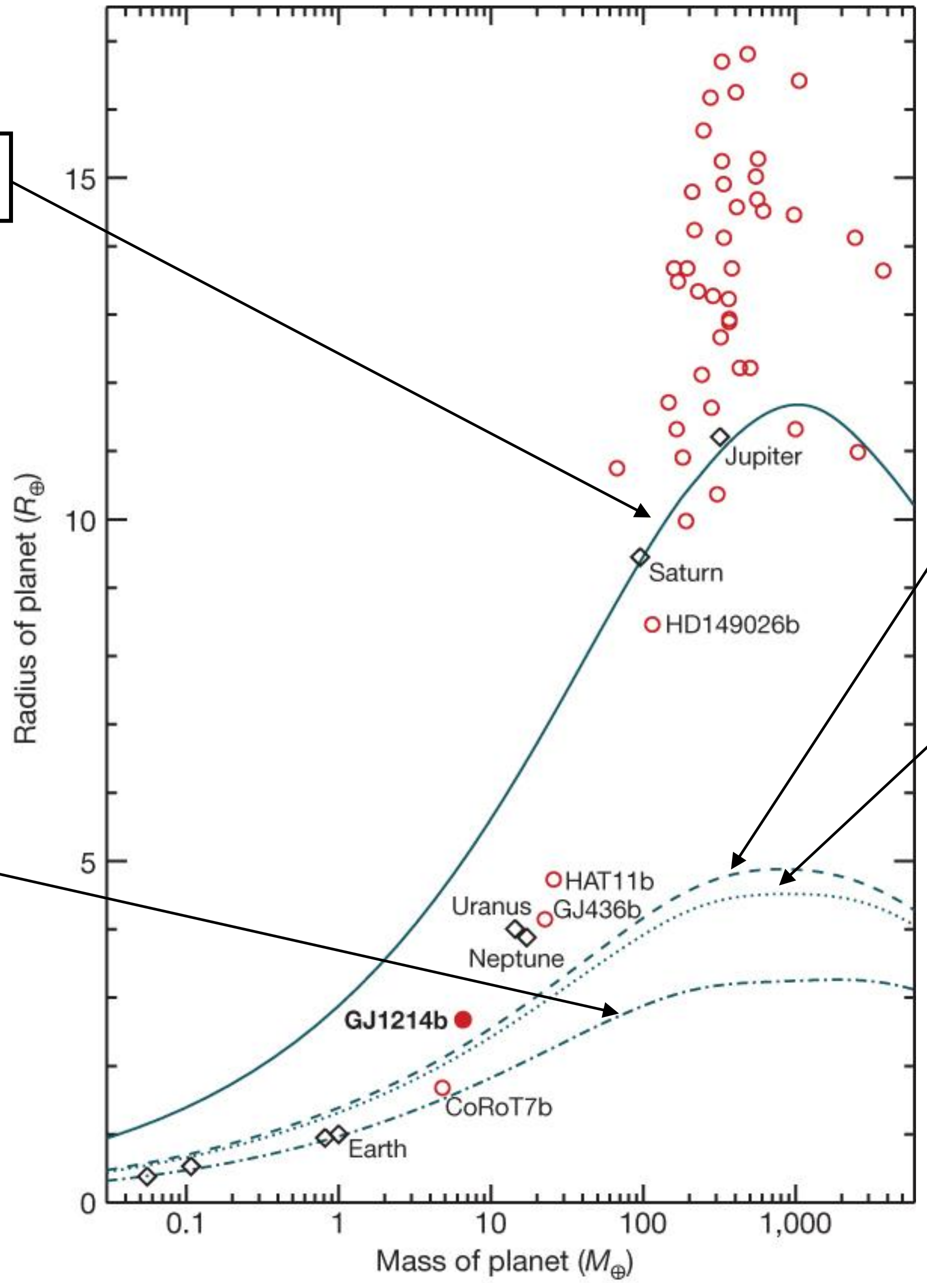

H/He dominated

Pure H_20

75% H_20,
22% Si

67.5% Si mantle
32.5% Fe
(earth-like)

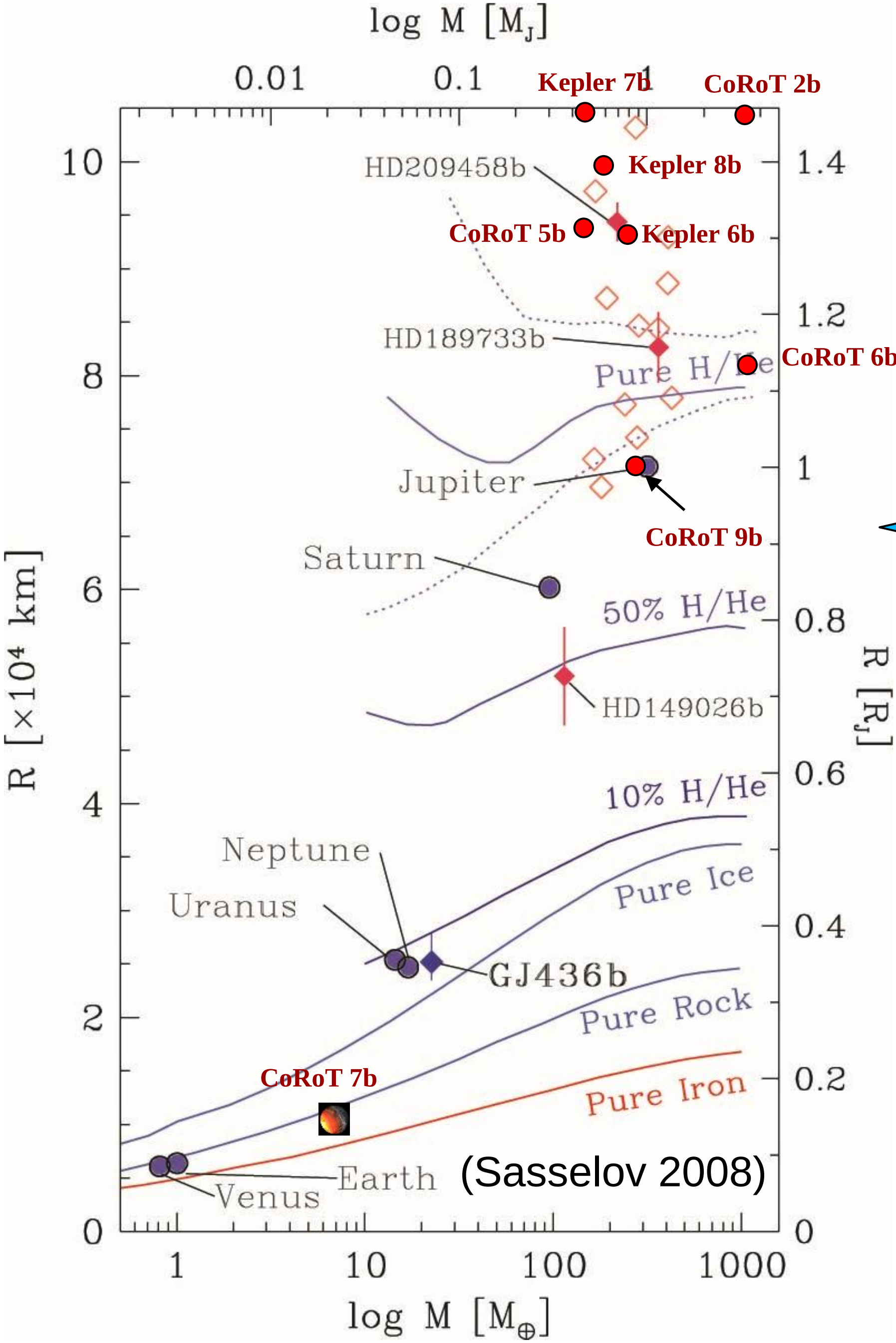

The mass-radius relationship of planets depends on their mass, composition and inner structure

Cold & Hot Jupiters

Hot Neptunes

Super Earths

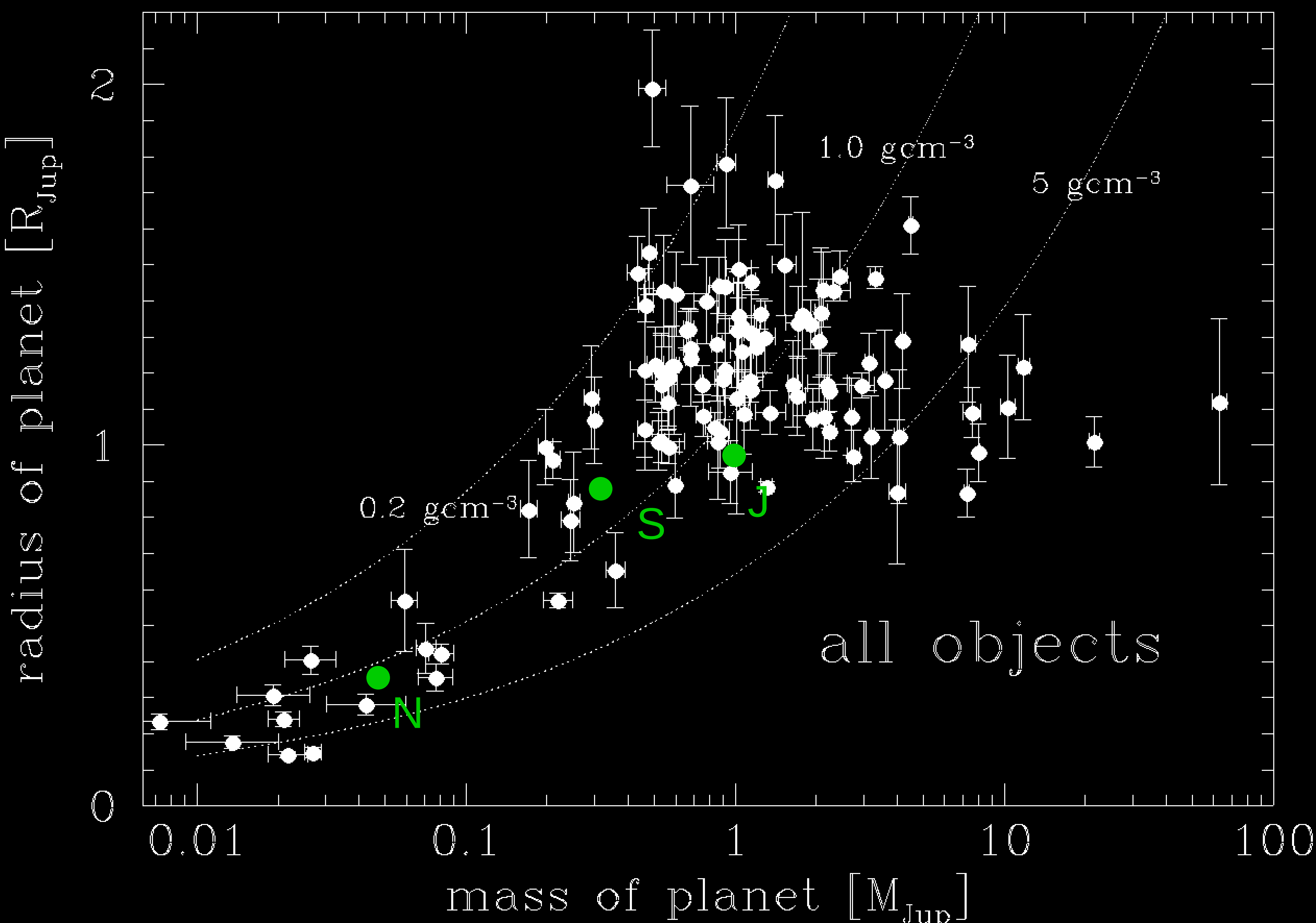

radius of planet [R_{Jup}]
2
1
0
0.01
0.1
1
10
100
mass of planet [M_{Jup}]
0.2 gcm^{-3}
1.0 gcm^{-3}
5 gcm^{-3}
N
S
J
all objects

HD 149026: A planet with a large core

Sato et al. 2005

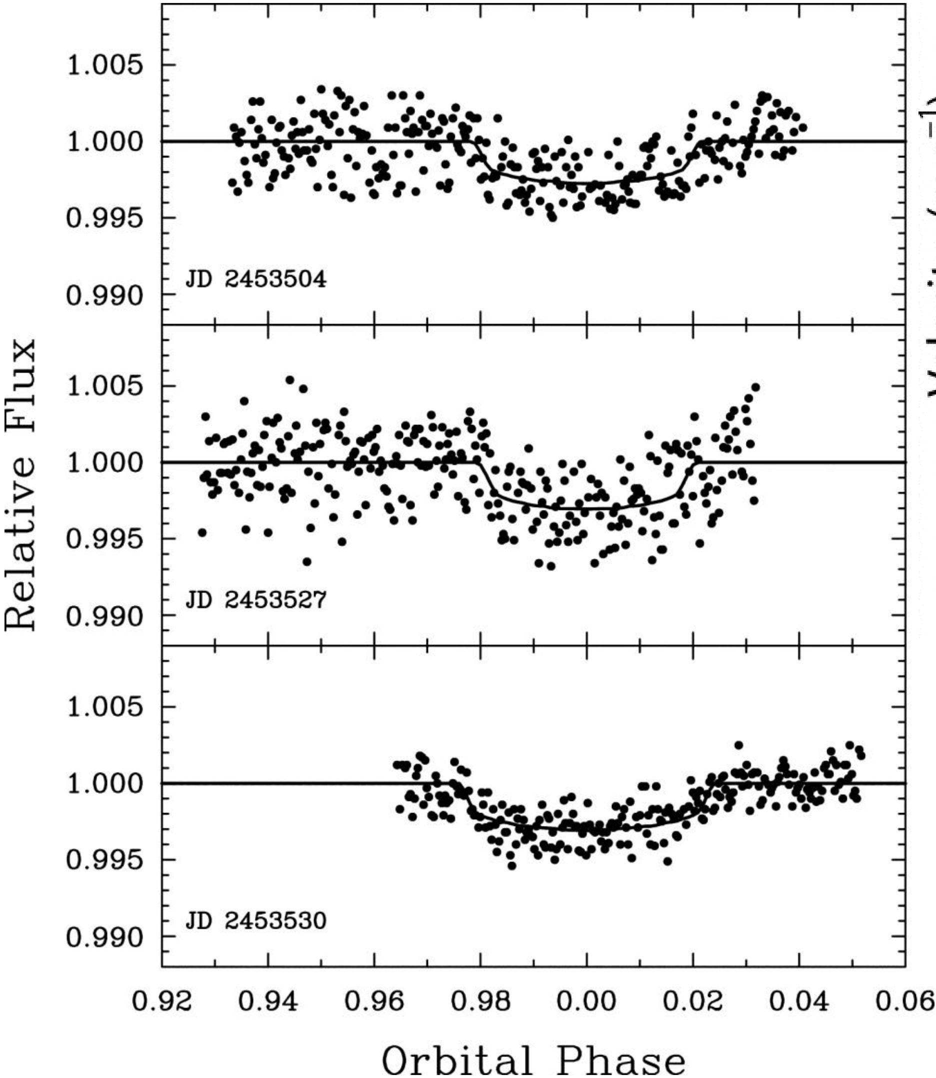

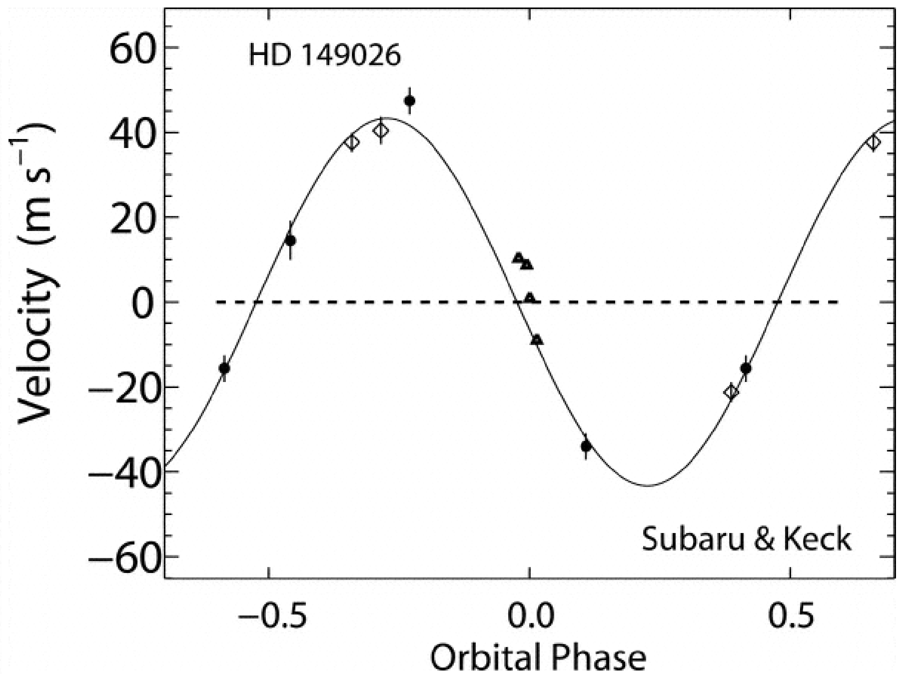

Period = 2.87 d

$R_p = 0.7\ R_{Jup}$

$M_p = 0.36\ M_{Jup}$

Mean density = 2.8 gm/cm^3

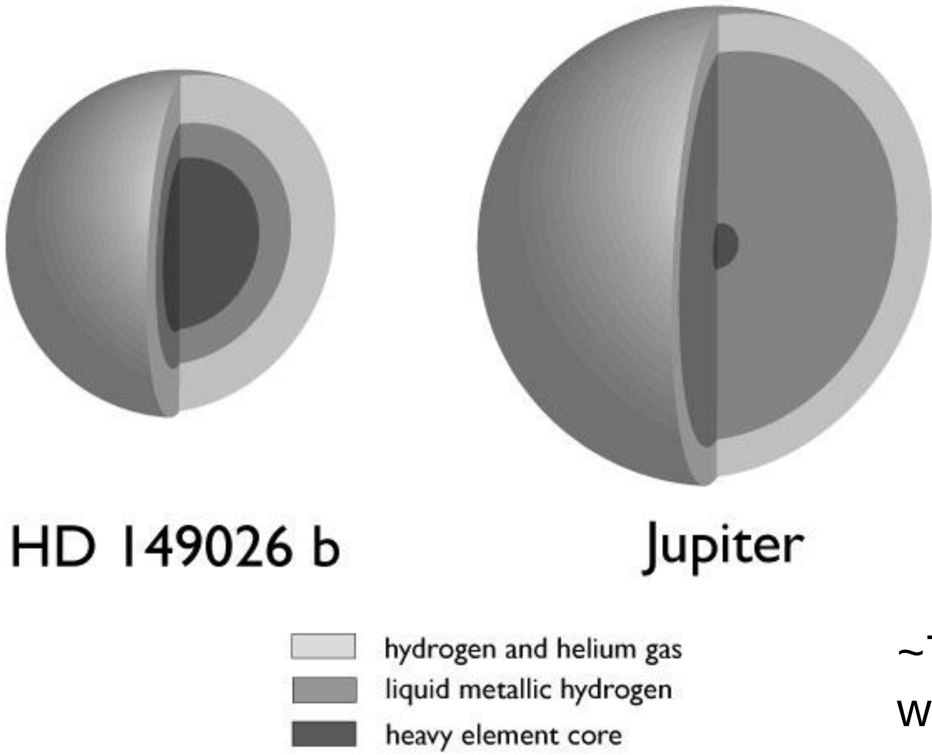

10-13 M_{earth} core

~70 M_{earth} core mass is difficult to form with gravitational instability.

HD 149026 b provides strong support for the **core accretion theory**

TABLE 6
Model Radius and Core Mass

Radius (R_J, Equatorial)		Core Mass
$\rho_c = 10.5$ g cm^{-3}	$\rho_c = 5.5$ g cm^{-3}	($M_\oplus$)
0.594	0.662 (C)	89.3
0.681 (A)	0.745 (D)	74.5
0.769 (B)	0.818	60.0
0.866	0.905	43.6

Note.—A–B and C–D bracket the interpolated core masses for the respective ρ_c (see § 5).

$R_p = 0.7\ R_{Jup}$

$M_p = 0.36\ M_{Jup}$

Mean density = 2.8 gm/cm^3

Planet Radius

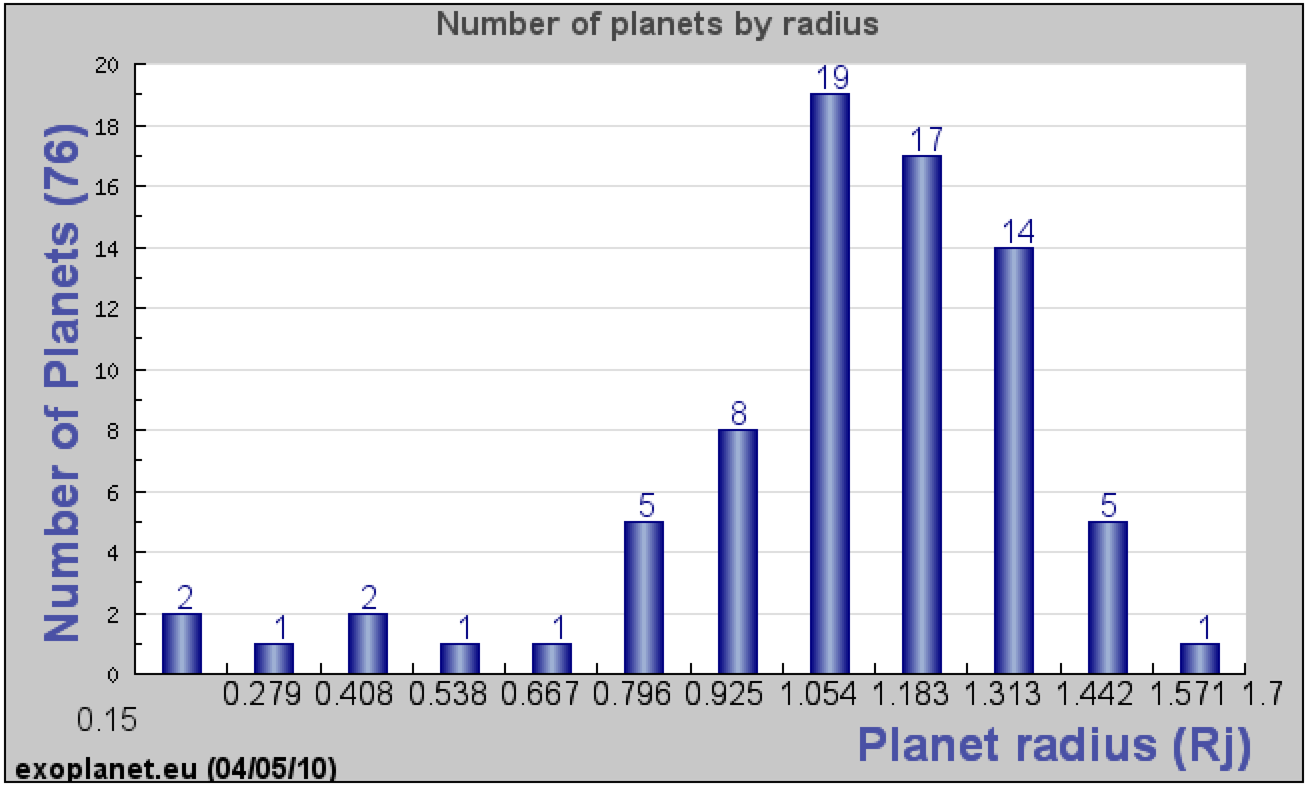

Most transiting planets tend to be inflated. Approximately 68% of all transiting planets have radii larger than 1.1 R_{Jup}.

Possible Explanations for the Large Radii

1. Irradiation from the star heats the planet and slows its contraction it thus will appear „younger“ than it is and have a larger radius

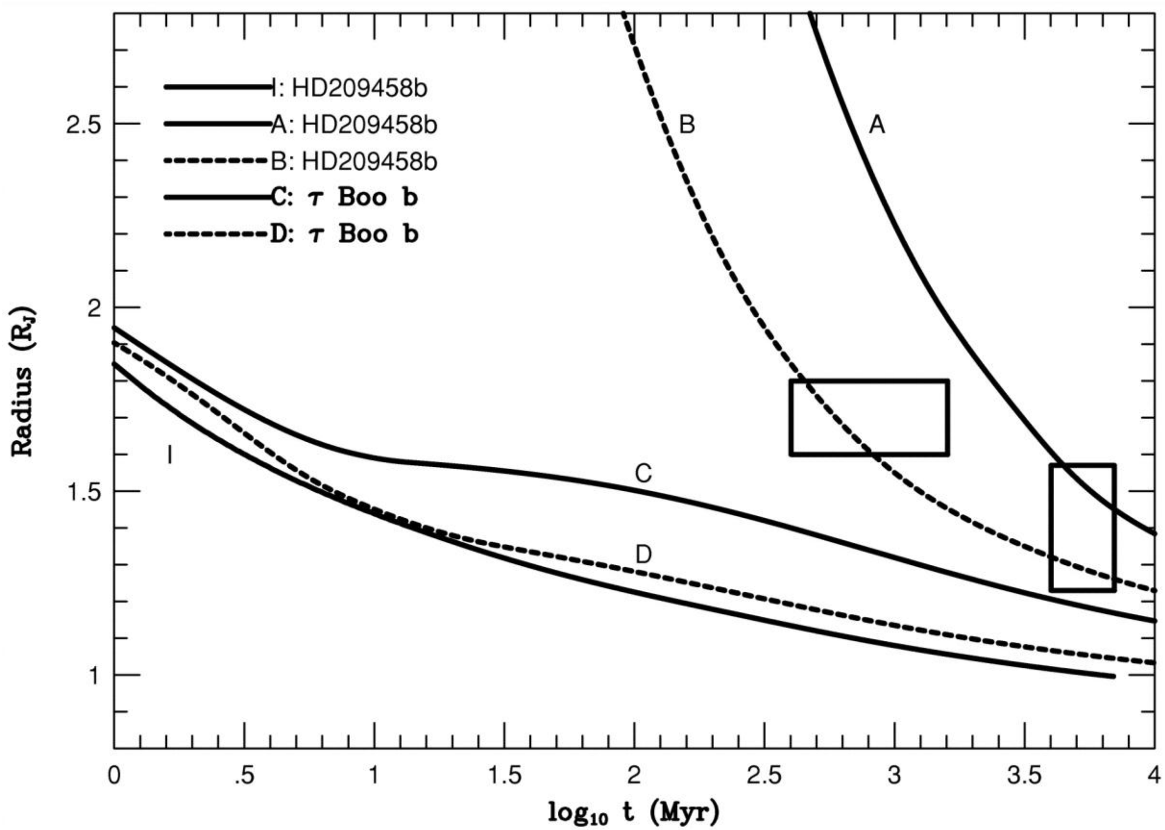

Possible Explanations for the Large Radii

2. Slight orbital eccentricity (difficult to measure) causes tidal heating of core → larger radius

Slight Problem:

HD 17156b: e=0.68 $R = 1.02\ R_{Jup}$

HD 80606b: e=0.93 $R = 0.92\ R_{Jup}$

CoRoT 10b: e=0.53 $R = 0.97 R_{Jup}$

Caveat: These planets all have masses 3-4 M_{Jup}, so it may be the smaller radius is just due to the larger mass.

3. We do not know what is going on.

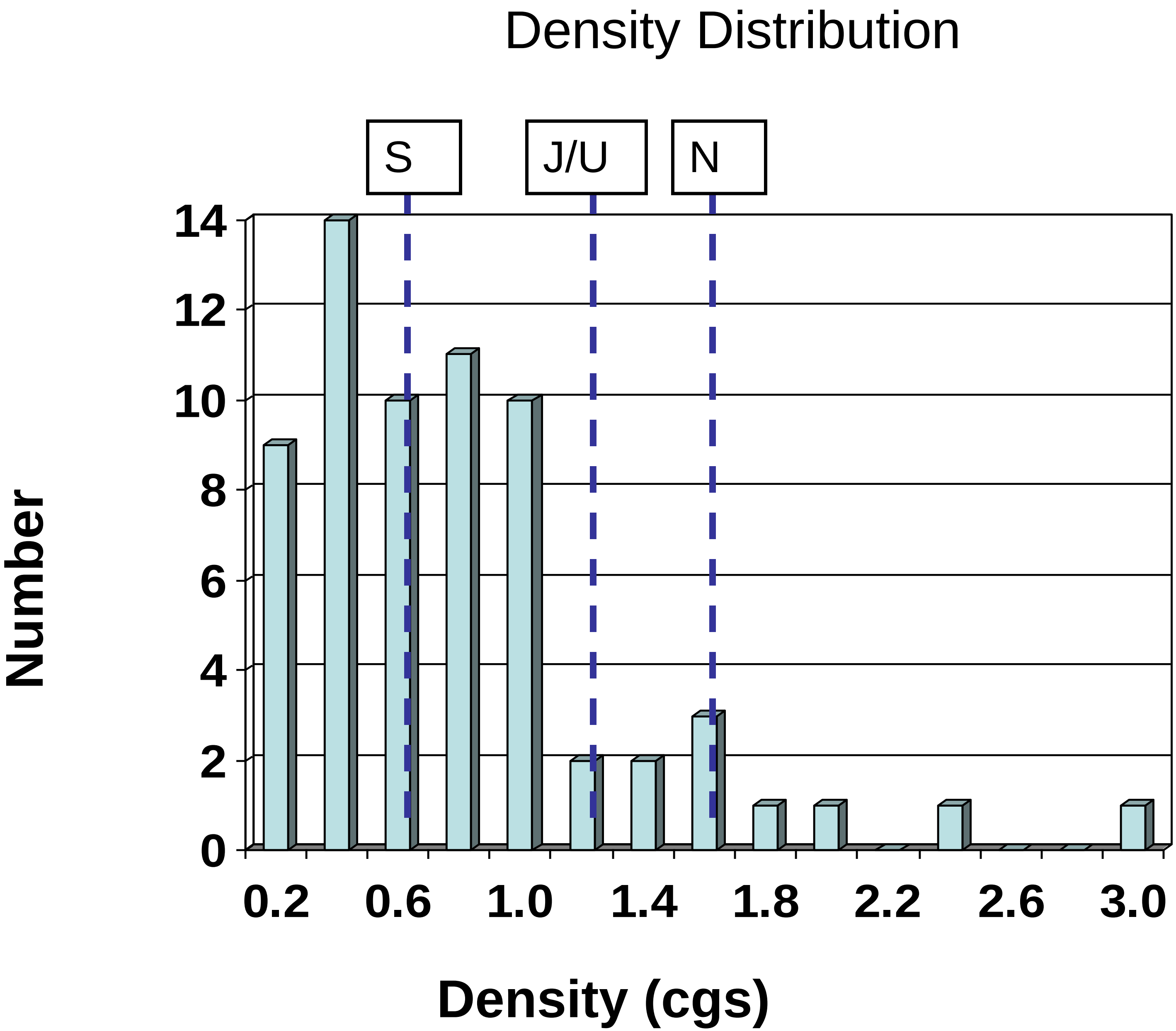
Density Distribution
S
J/U
N
Number
0
2
4
6
8
10
12
14
0.2
0.6
1.0
1.4
1.8
2.2
2.6
3.0
Density (cgs)

Comparison of Mean Densities

Giant Planets with $M < 2\ M_{Jup}$: 0.78 cgs

HD 17156, P = 21 d, e= 0.68 M = 3.2 M_{Jup}, density = 3.8

HD 80606, P = 111 d, e=0.93, M = 3.9 M_{Jup}, density = 6.4

CoRoT 10b, P=13.2, e= 0.53, M = 2.7 M_{Jup}, density = 3.7

CoRoT 9b, P = 95 d, e=0.12, M = 1 M_{Jup}, density = 0.93

The three eccentric transiting planets have high mass and high densities. Formed by mergers?

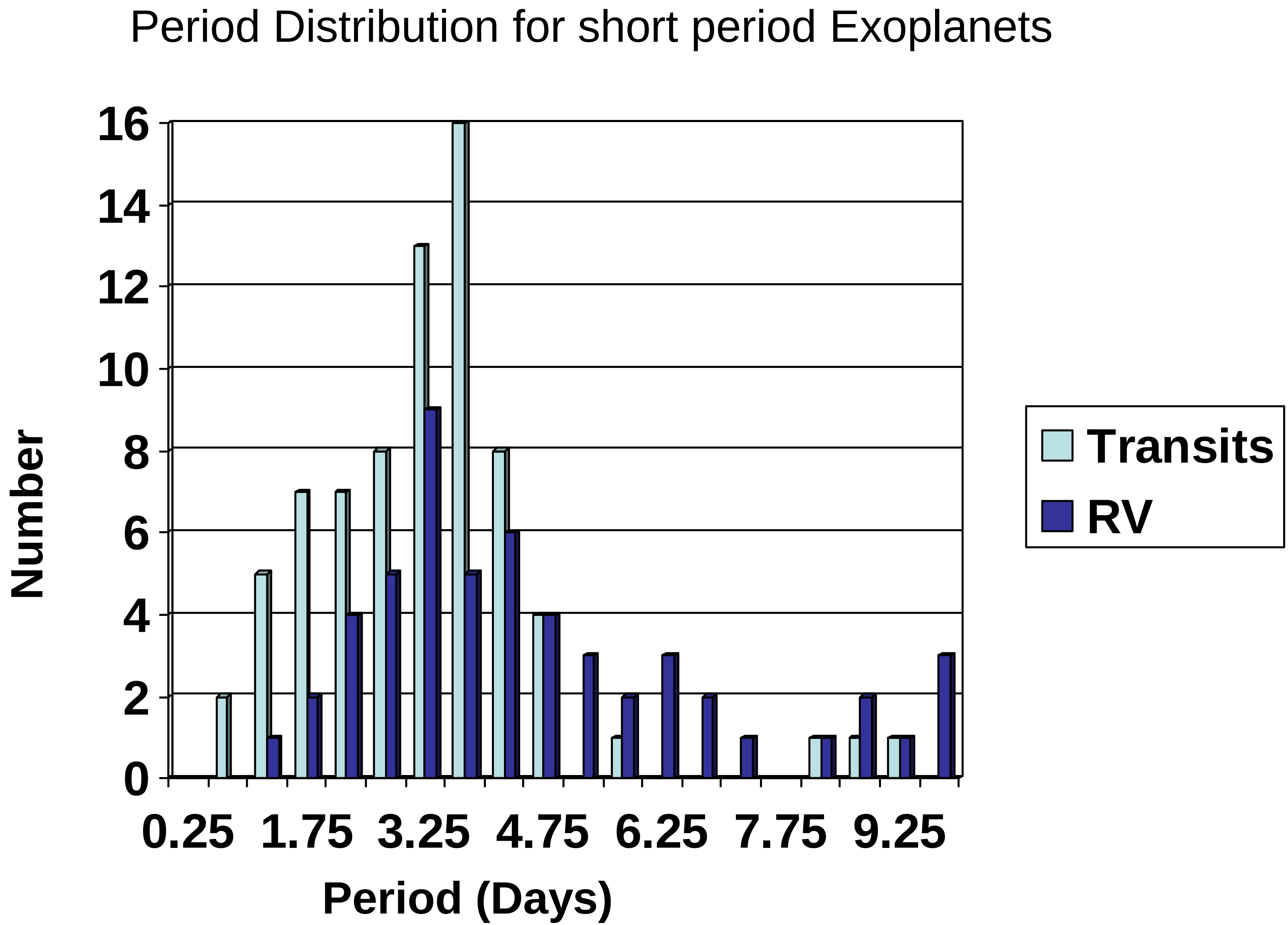
Period Distribution for short period Exoplanets
Number
16
14
12
10
8
6
4
2
0
0.25
1.75
3.25
4.75
6.25
7.75
9.25
Period (Days)
Transits
RV

Both RV and Transit Searches show a peak in the Period at 3 days

The ≈ 3 day period may mark the inner edge of the proto-planetary disk, => where migration stops?

Mass-Radius Relationship

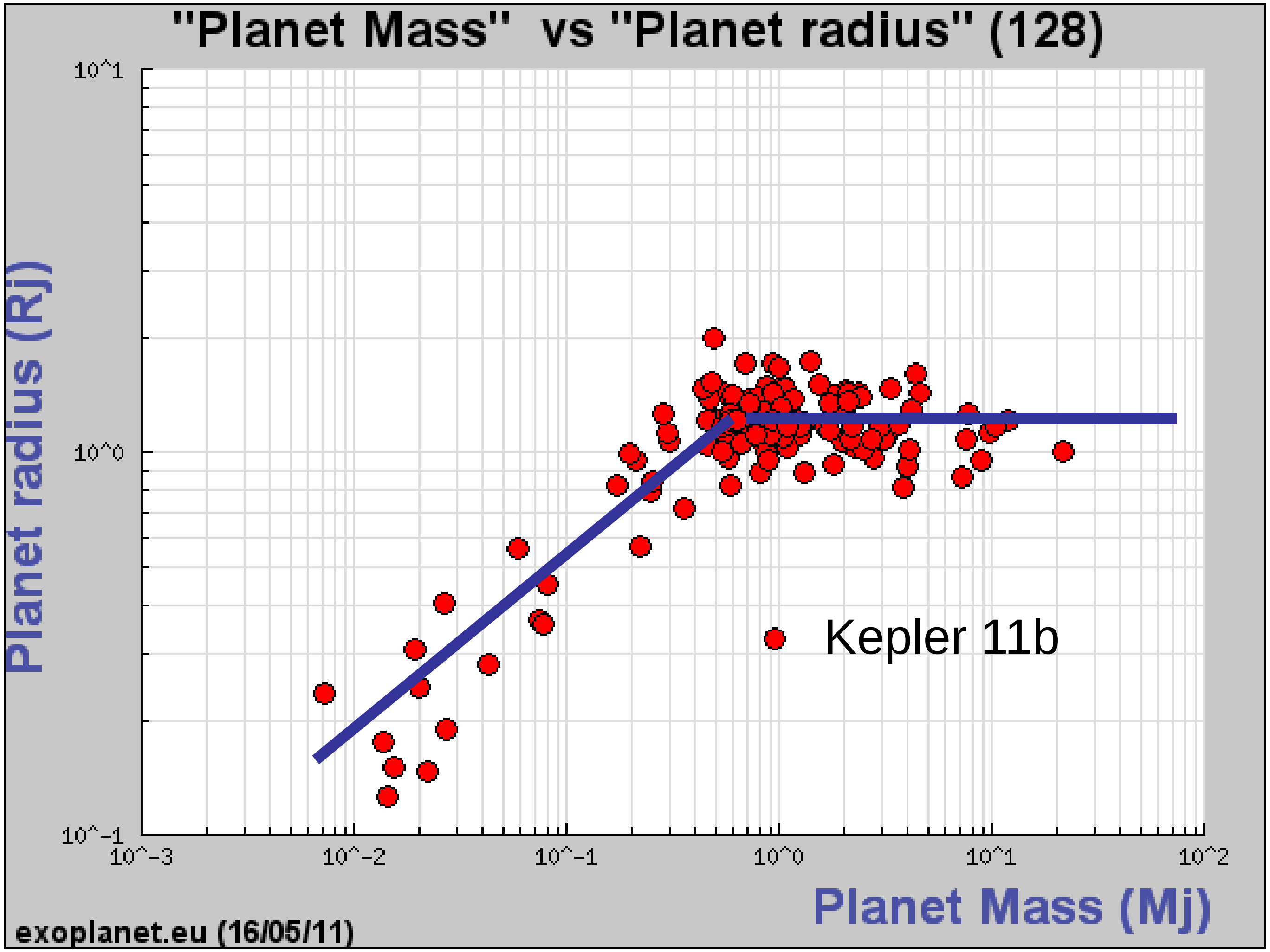

Radius is roughly independent of mass, until you get to small planets (rocks)

Planet Mass Distribution

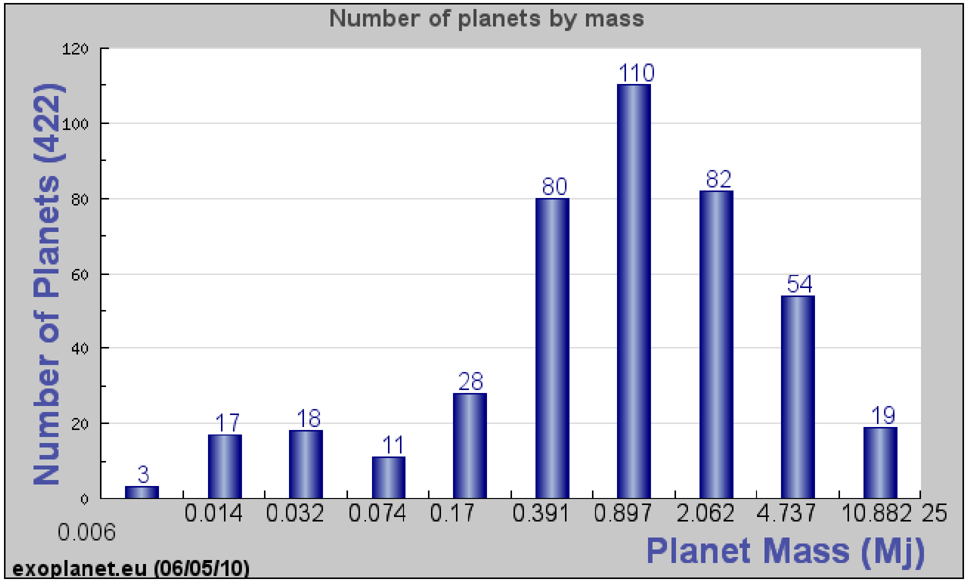

RV Planets

Close in planets tend to have lower mass, as we have seen before.

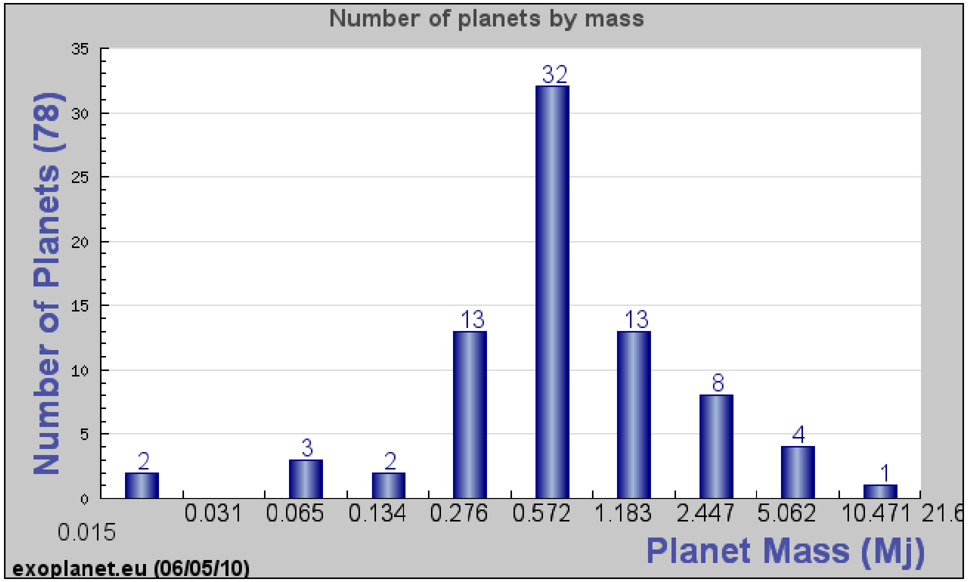

Transiting Planets

Host Star Mass Distribution

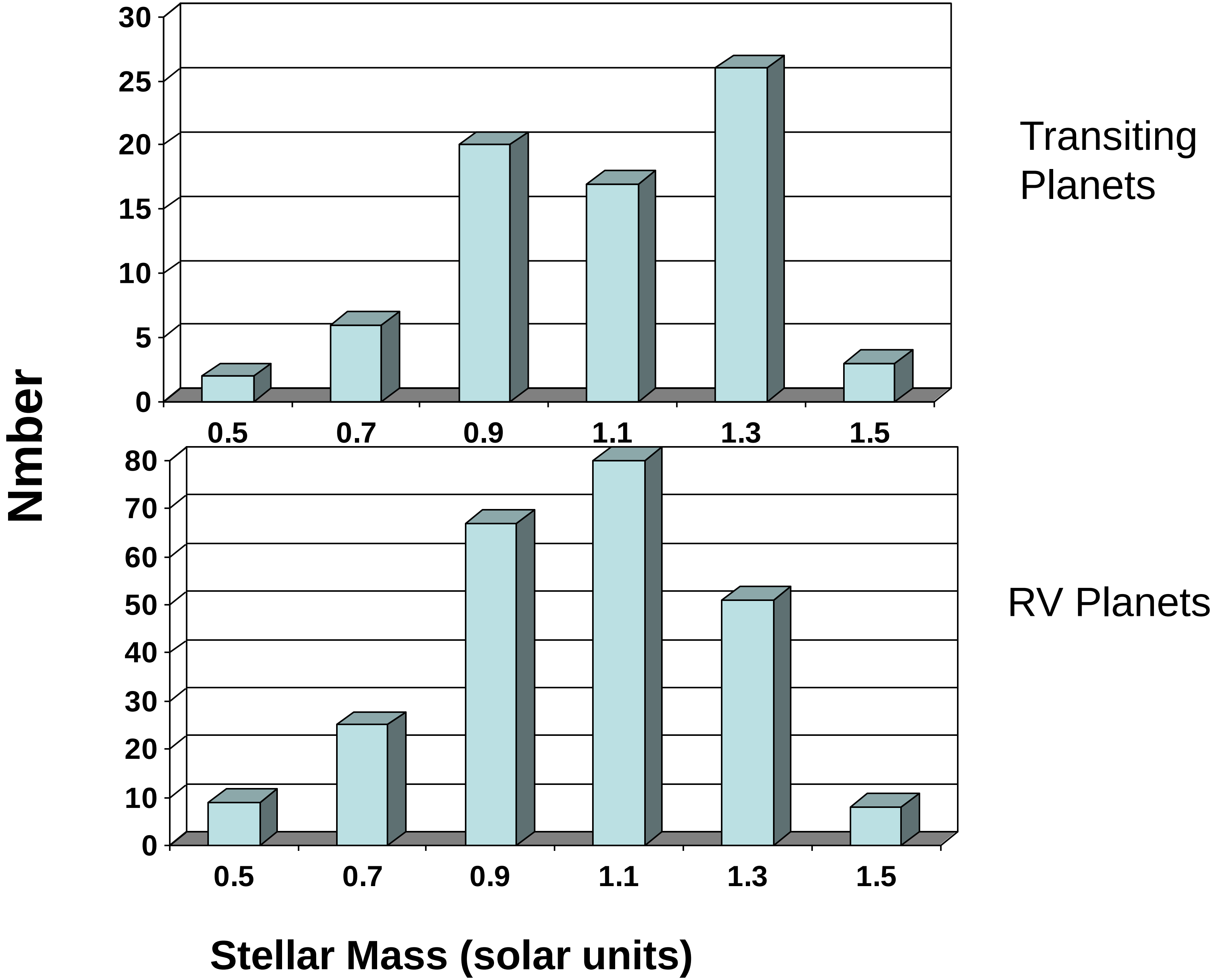

Stellar Magnitude distribution of Exoplanet Discoveries

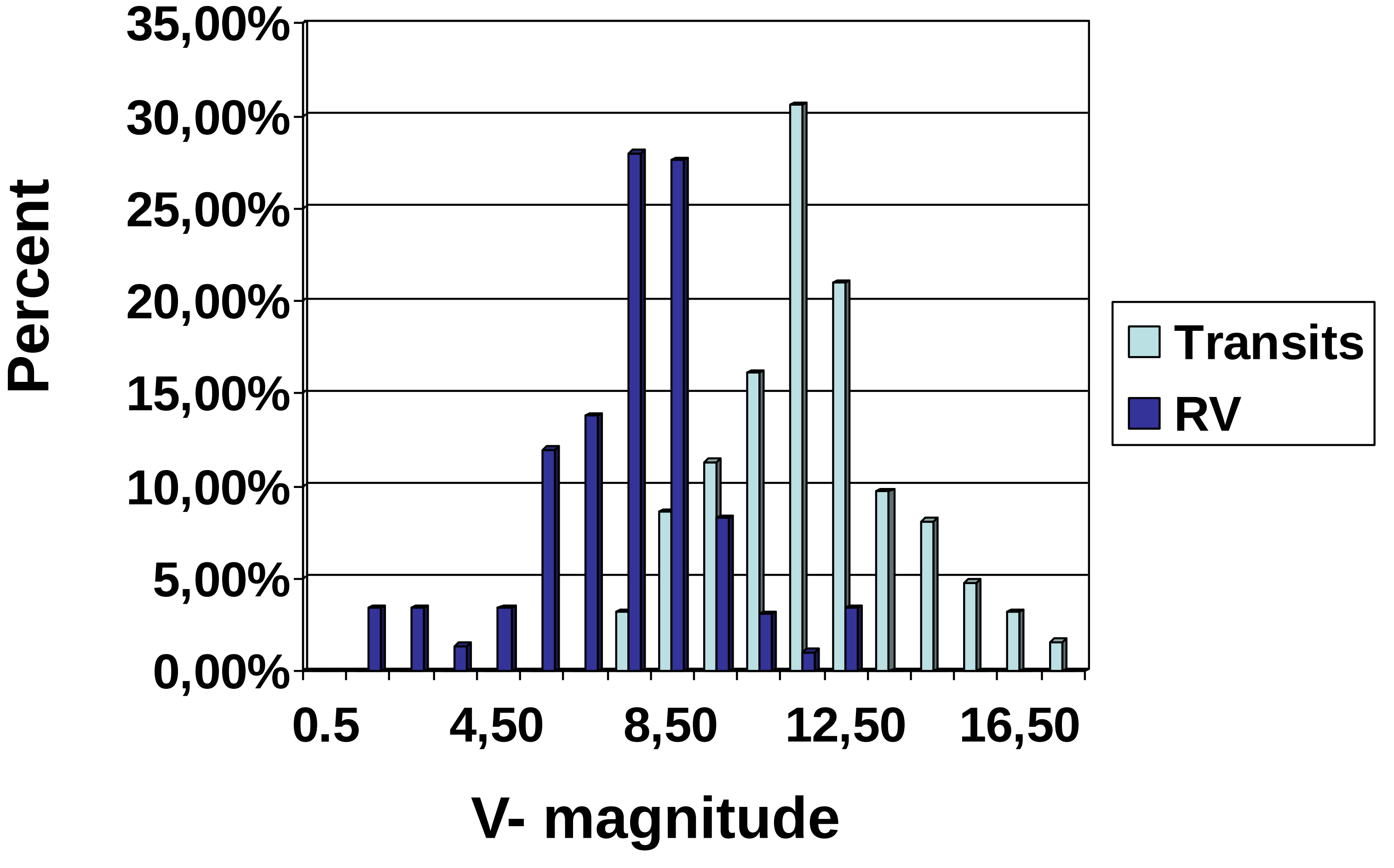

Summary of Global Properties of Transiting Planets

1. Mass – Radius Diagram !!!! => internal composition
2. Transiting giant planets (close-in) tend to have inflated radii (much larger than Jupiter)
3. A significant fraction of transiting giant planets are found around early-type stars with masses ≈ 1.3 M_{sun}.
4. The period distribution of close-in planets peaks around P ≈ 3 days.
5. Most transiting giant planets have densities near that of Saturn. It is not known if this is due to their close proximity to the star (i.e. inflated radius)
6. Transiting planets have been discovered around stars fainter than those from radial velocity surveys

- Early indications are that the host stars of transiting planets have different properties than non-transiting planets (more details later).

- Most likely explanation: Transit searches are not as biased as radial velocity searches. One looks for transits around all stars in a field, these are not pre-selected. The only bias comes with which ones are followed up with Doppler measurements

- Caveat: Transit searches are biased against smaller stars. i.e. the larger the star the higher probability that it transits

The Rossiter-McClaughlin Effect

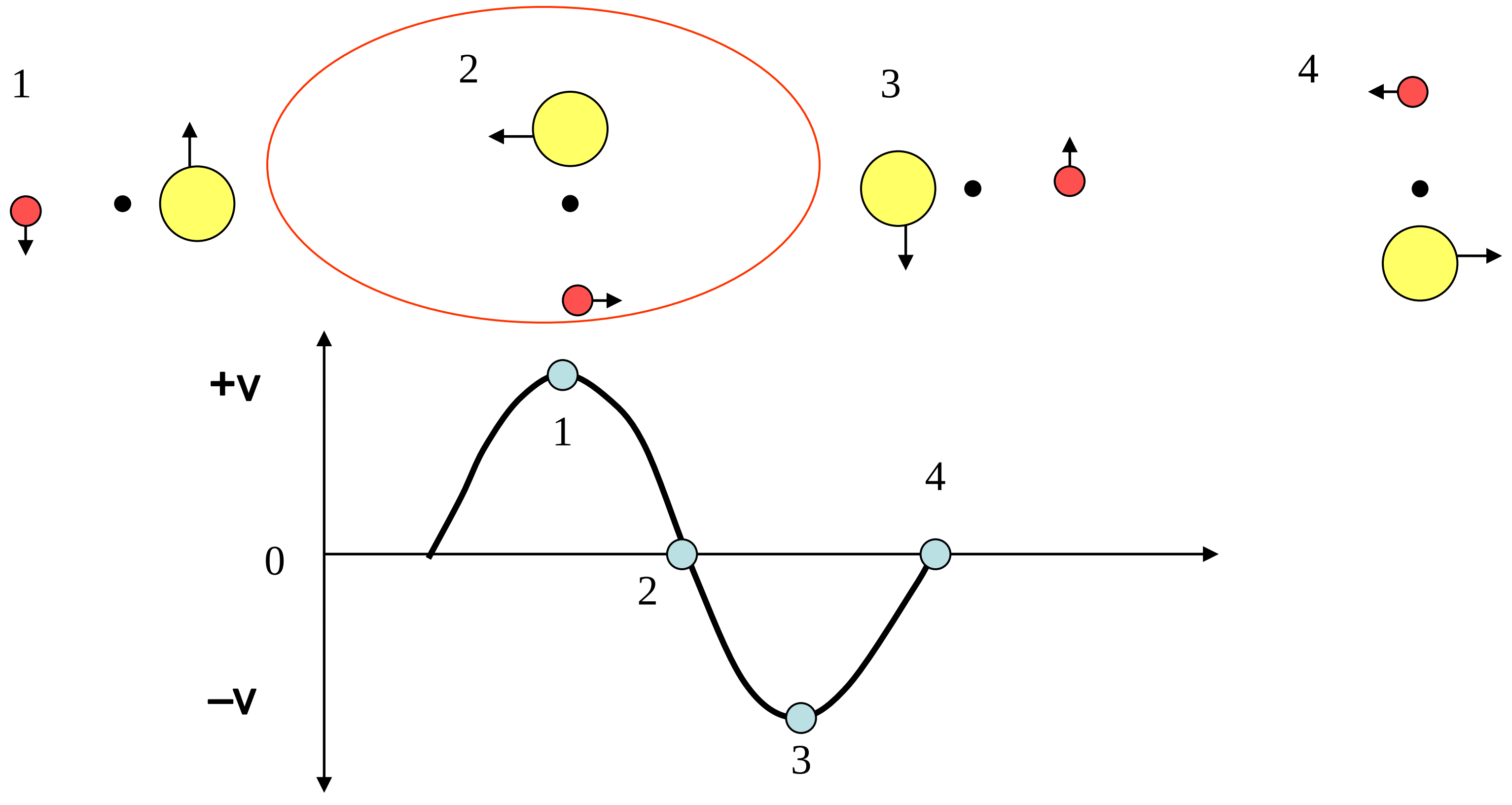

The R-M effect occurs in eclipsing systems when the companion crosses in front of the star. This creates a distortion in the normal radial velocity of the star. This occurs at point 2 in the orbit.

The effect was discovered in 1924 independently by Rossiter and McClaughlin

ON THE DETECTION OF AN EFFECT OF ROTATION DURING ECLIPSE IN THE VELOCITY OF THE BRIGHTER COMPONENT OF BETA LYRAE, AND ON THE CONSTANCY OF VELOCITY OF THIS SYSTEM

By R. A. ROSSITER

ABSTRACT

The spectroscopic velocity of the Beta Lyrae system.—Elements from a series of spectrograms taken at the Allegheny Observatory in 1907 and from seven series, comprising a total of 442 spectrograms, taken at Ann Arbor in the years 1911 to 1921, show that the velocity of the center of mass of the system is constant and that elliptical motion is very well satisfied. Probably no third body exists, since no disturbance of the two-body system can be detected. The accompanying elliptic velocity curve, with radial velocities indicated by the large dots, shows how well elliptical motion is satisfied.

The rotational effect.—A secondary oscillation confined to the region of the velocity curve extending 1.6 days on each side of the principal minimum (or center of the eclipse of the small bright body by the large faint body) has been isolated from the orbital velocity and measured. It has been shown to be due to the velocity of rotation of the partially eclipsed smaller component, and is here termed the rotational effect. In Beta Lyrae it has a total range of 26 kilometers. A graphical determination of this curve of rotational velocity from Shapley's light-elements of Beta Lyrae gives a duration of eclipse 40 per cent longer than the spectroscope has shown and an amplitude correspondingly too great. Further investigation of this subject is under way.

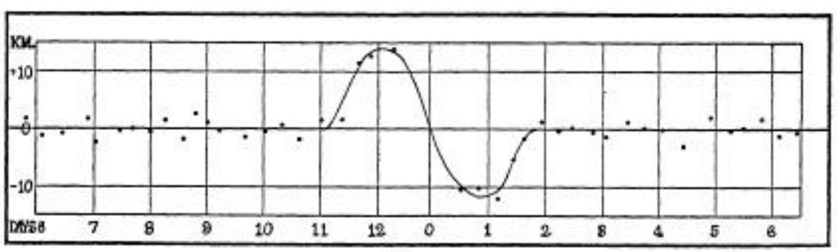

FIG. 2

Curves show Radial Velocity after removing the binary orbital motion

SOME RESULTS OF A SPECTROGRAPHIC STUDY OF THE ALGOL SYSTEM

By DEAN B. McLAUGHLIN

ABSTRACT

One hundred and fifty-six plates taken in 1913, 1920, and 1923 with the one-prism spectrograph of the Detroit Observatory form the basis of this discussion.

Short- and long-period orbits.—From plates taken within one month in 1923 orbital elements of the eclipsing system are determined. The value of $a \sin i$ is larger than in previous determinations. With these elements as standard the velocity of the center of mass is derived for other epochs by means of simple residuals. A period of about 1.885 years and a range of 20 km are indicated for the variation of the velocity of the center of mass of the eclipsing system, substantially in agreement with the determination by R. H. Curtiss.

Rotational effect.—This effect due to the rotation of the brighter star during the partial eclipse, discovered by Dr. Rossiter in Beta Lyrae, is investigated in Algol and is found to have a range of 35 km as shown in the diagram. Computation with Stebbins' light-elements gives only half the observed range of the effect, on assumption that $m_b = 2m_f$. Investigation of this rotational effect is suggested as a means of determining dimensions of other eclipsing systems. Agreement of form of computed and observed curves serves as a check on light-elements.

Dimensions of the eclipsing system.—Assuming equal periods of revolution and rotation of the bright star the dimensions of the eclipsing system are calculated. The total mass is 5.67 ☉. Mass ratio is $m_b = 5.0\, m_f$. Radii of the stars are: $r_b = 3.12$ ☉, and $r_f = 3.68$ ☉. Distance between centers: 10,522,000 km. Densities: $d_b = 0.16$, $d_f = 0.02$ (☉ = 1).

Parallax.—Hypothetical parallax of Algol is 0."031. Orbital motion is suggested as a possible cause of negative parallaxes of certain stars.

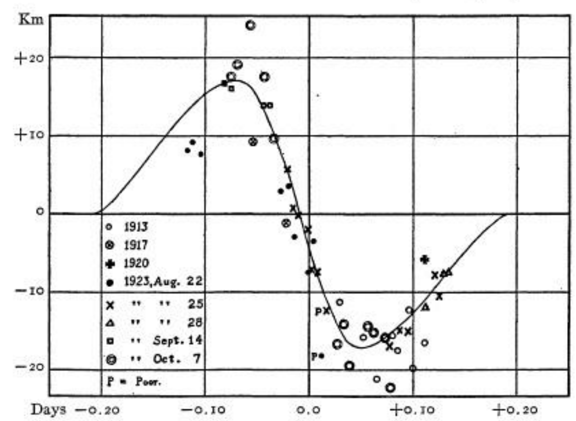

FIG. 1.—Curve of the rotational effect in Algol

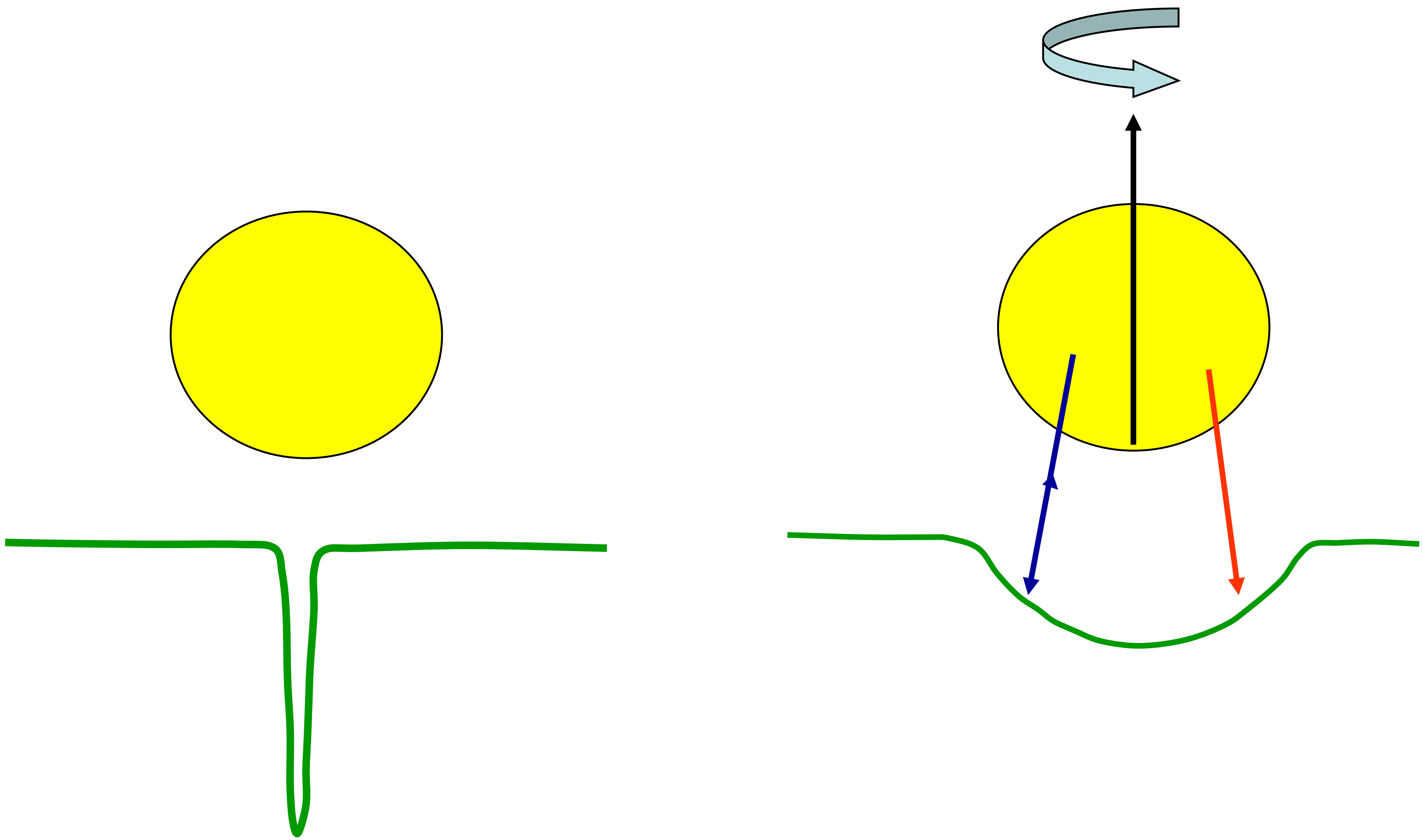

The Rossiter-McLaughlin Effect or „Rotation Effect“

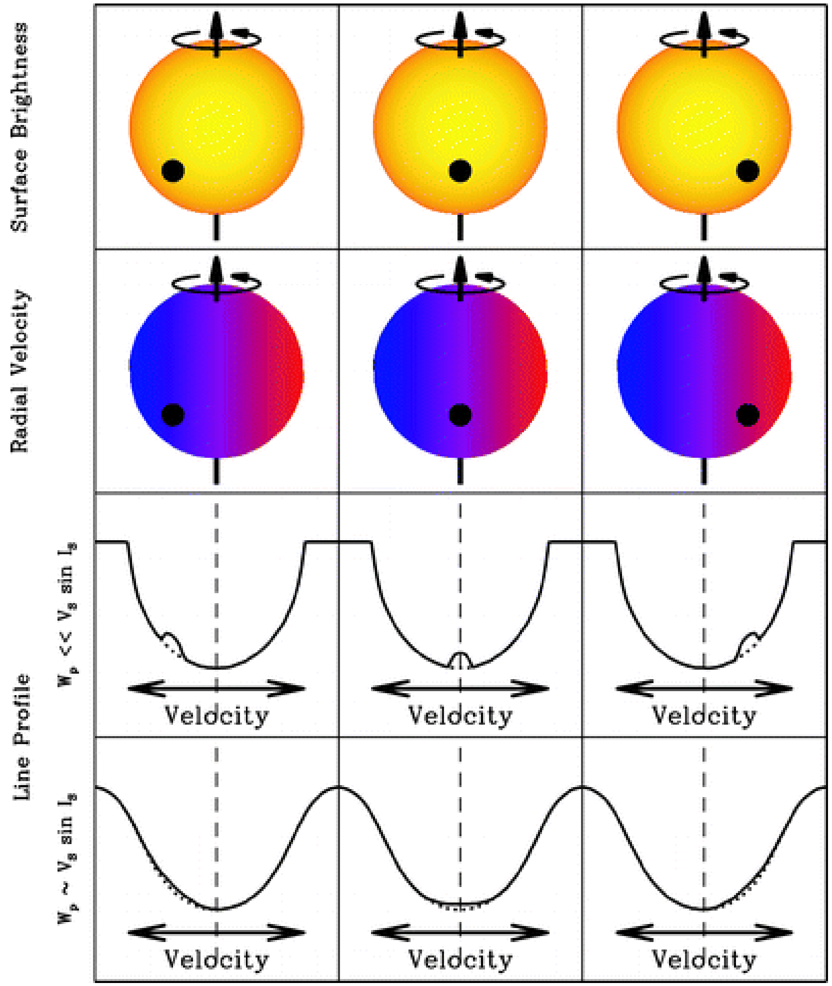

For rapidly rotating stars you can „see“ the planet in the spectral line

The Rossiter-McClaughlin Effect

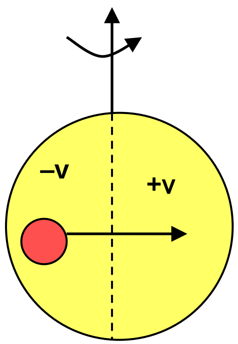

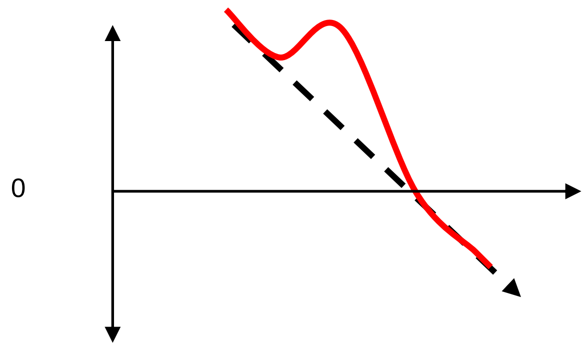

As the companion cosses the star the observed radial velocity goes from + to – (as the planet moves towards you the star is moving away). The companion covers part of the star that is rotating towards you. You see more positive velocities from the receeding portion of the star) you thus see a displacement to + RV.

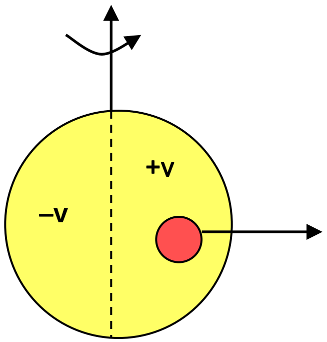

When the companion covers the receeding portion of the star, you see more negatve velocities of the star rotating towards you. You thus see a displacement to negative RV.

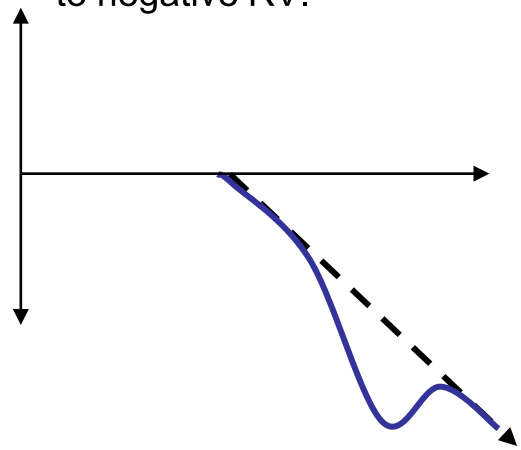

The Rossiter-McClaughlin Effect

What can the RM effect tell you?

1) The orbital inclination

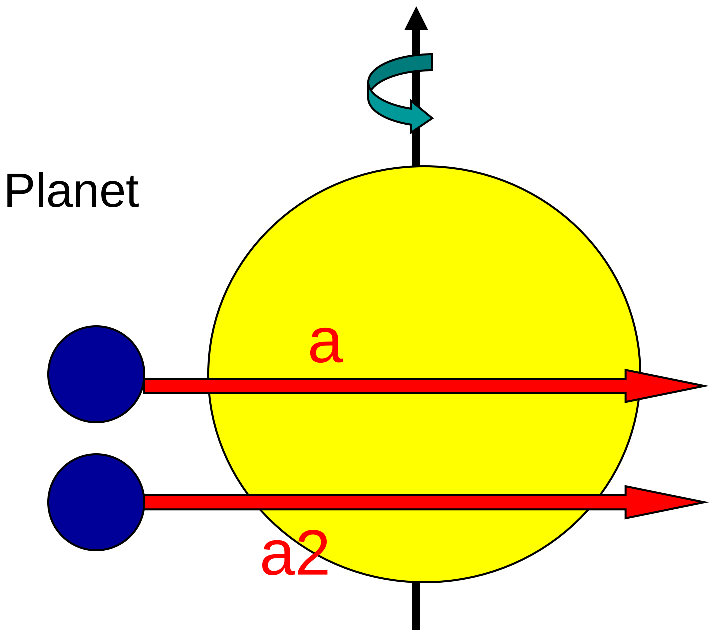

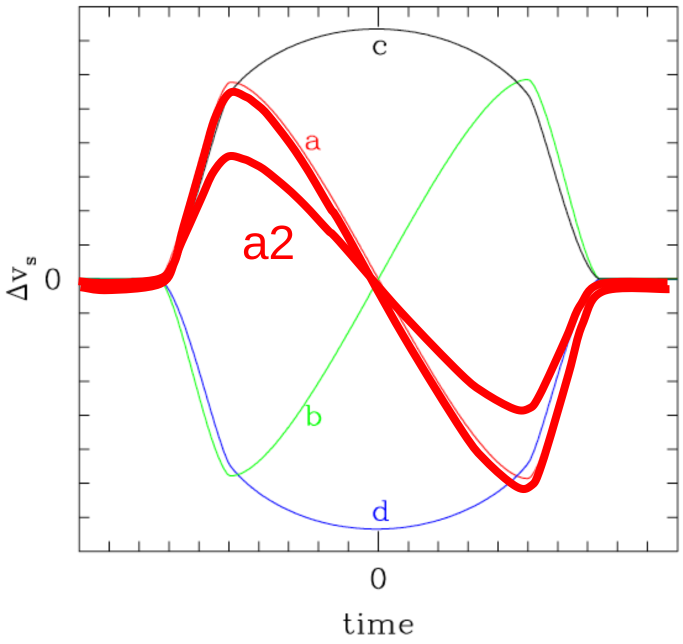

The Rossiter-McClaughlin Effect

2) The direction of the orbit

Planet

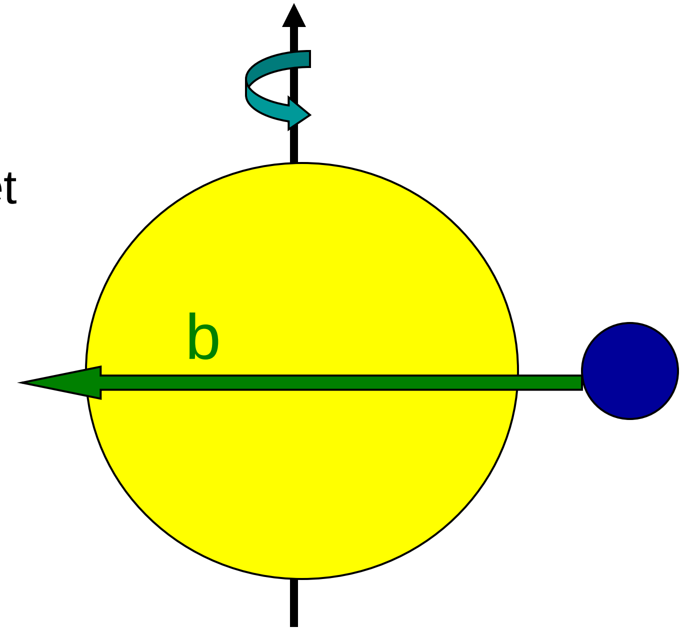

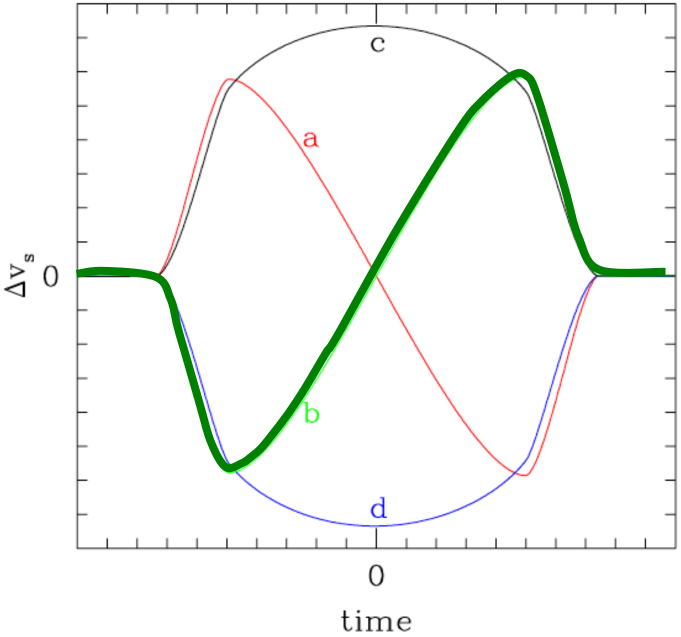

The Rossiter-McClaughlin Effect

2) The alignment of the orbit

Planet

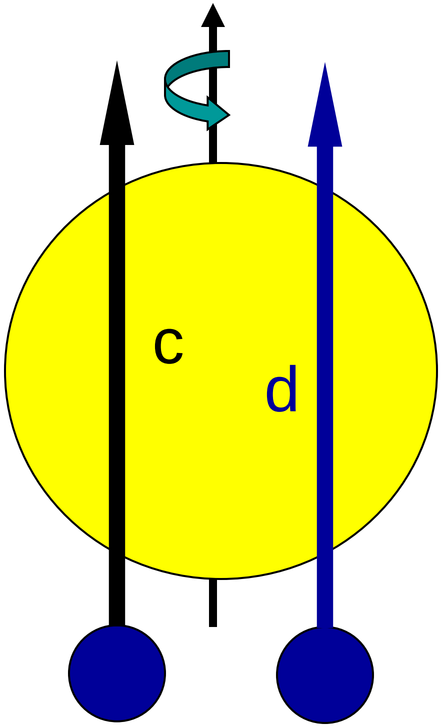

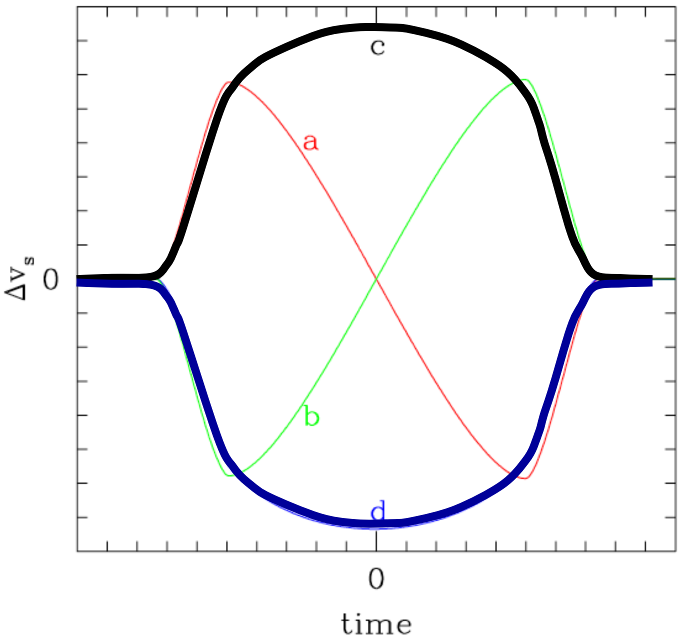

What can the RM effect tell you?

3. Are the spin axes aligned?

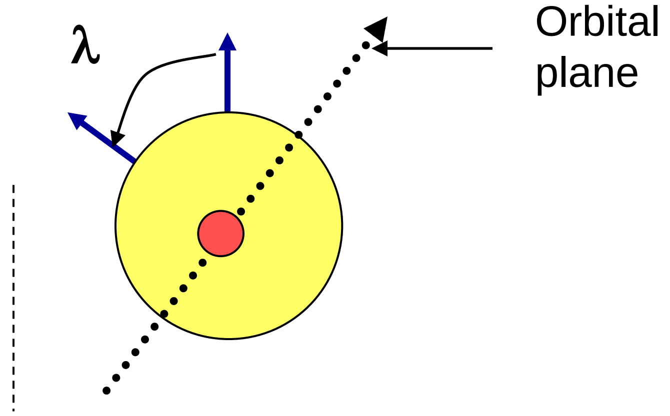

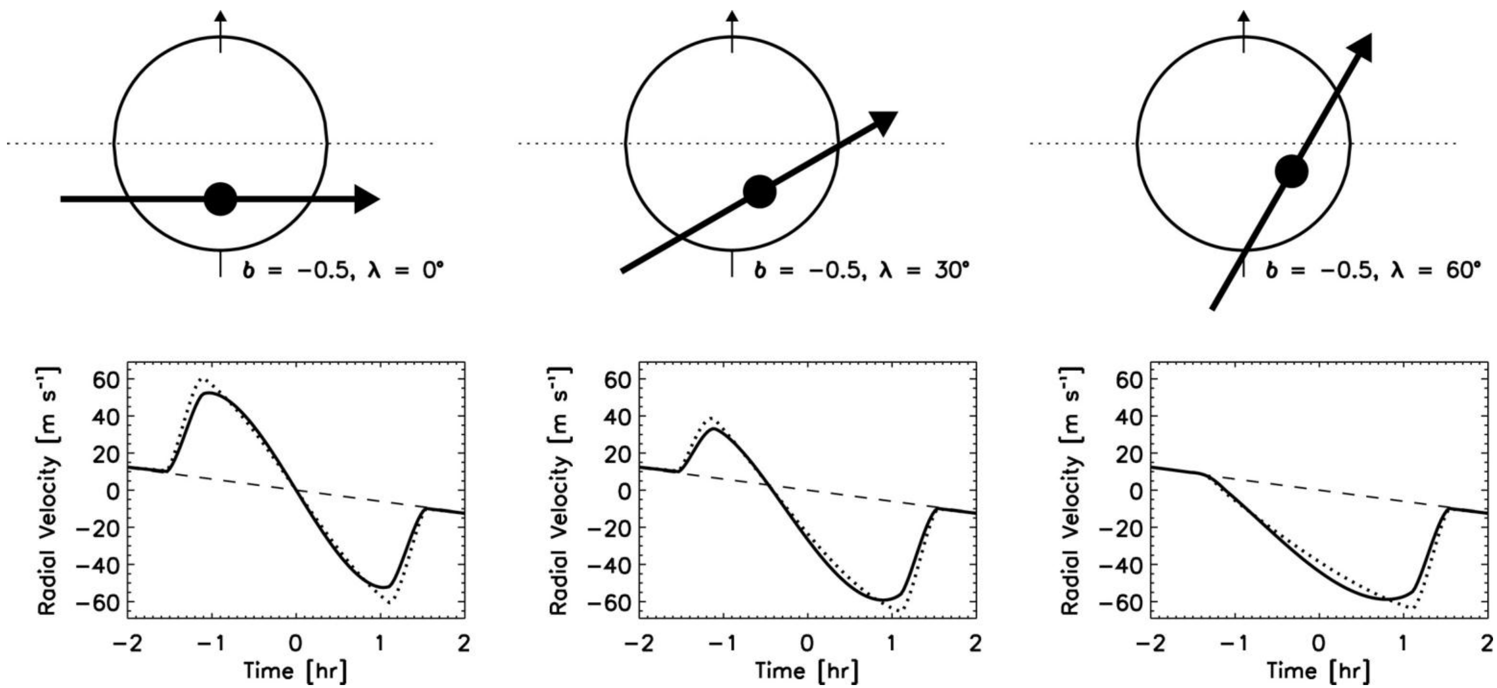

HD 209458

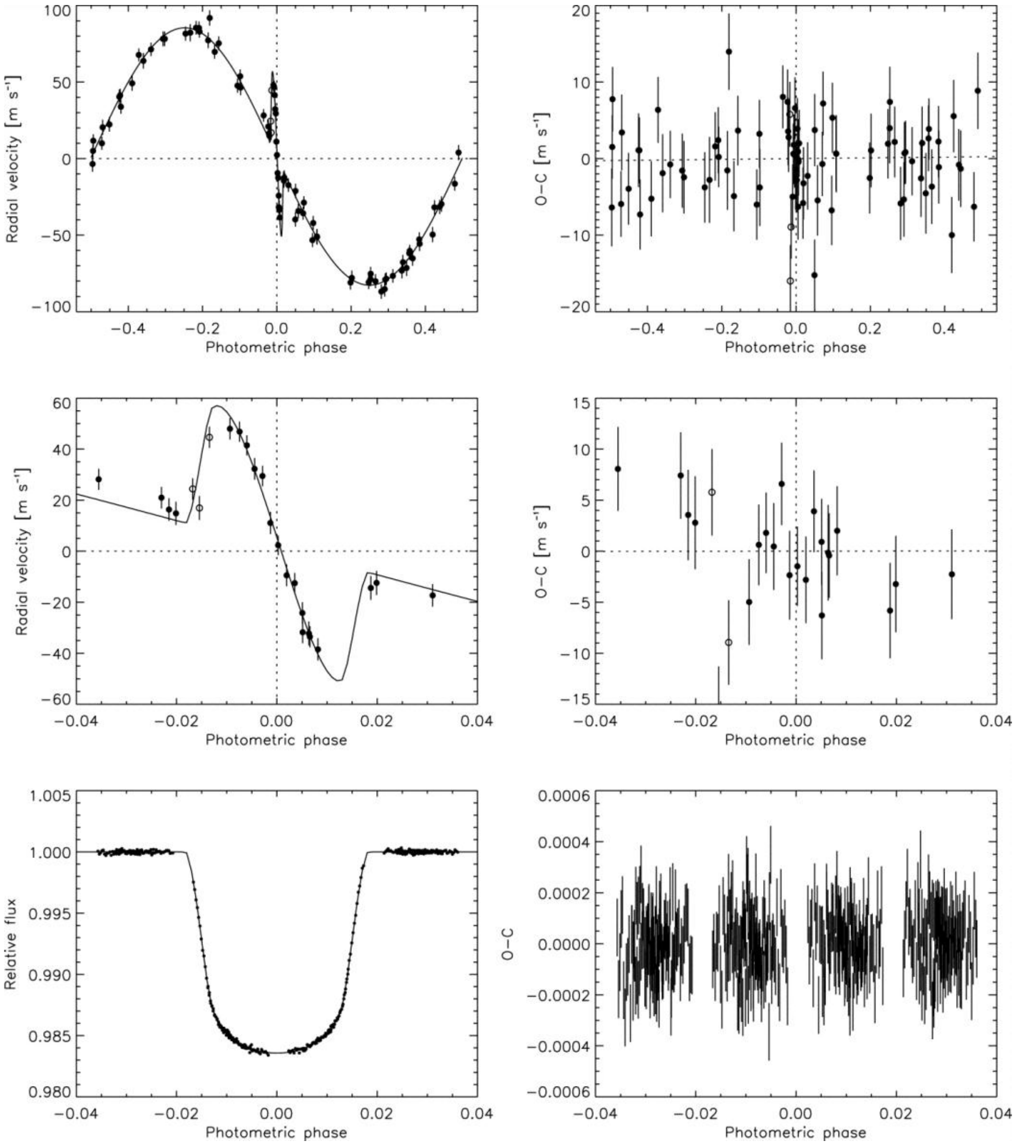

$\lambda = -0.1 \pm 2.4$ deg

What about HD 17156?

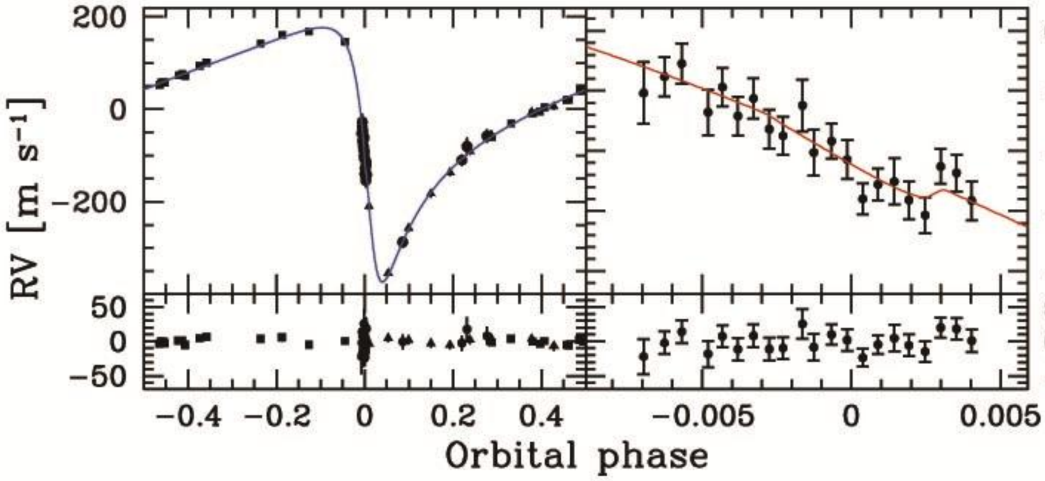

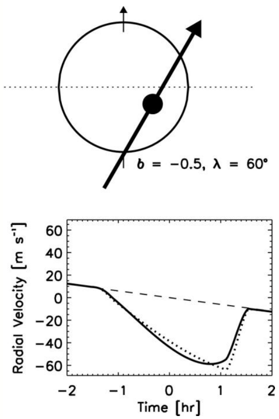

Fig. 2. Radial velocities of HD 17156 as a function of orbital phase, and the best-fitting model with the *a priori* constraint on $V \sin I_{\mathrm{S}}$. Three symbols represent the different data sets (circle, OAO; triangle, Subaru; square, Keck). Left panel: The entire orbit. Right panel: A zoom of transit phase. Bottom panels: Residuals from the best-fit curve.

Narita et al. (2007) reported a large (62 ± 25 degree) misalignment between planet orbit and star spin axes!

Cochran et al. 2008: λ = 9.3 ± 9.3 degrees → No misalignment!

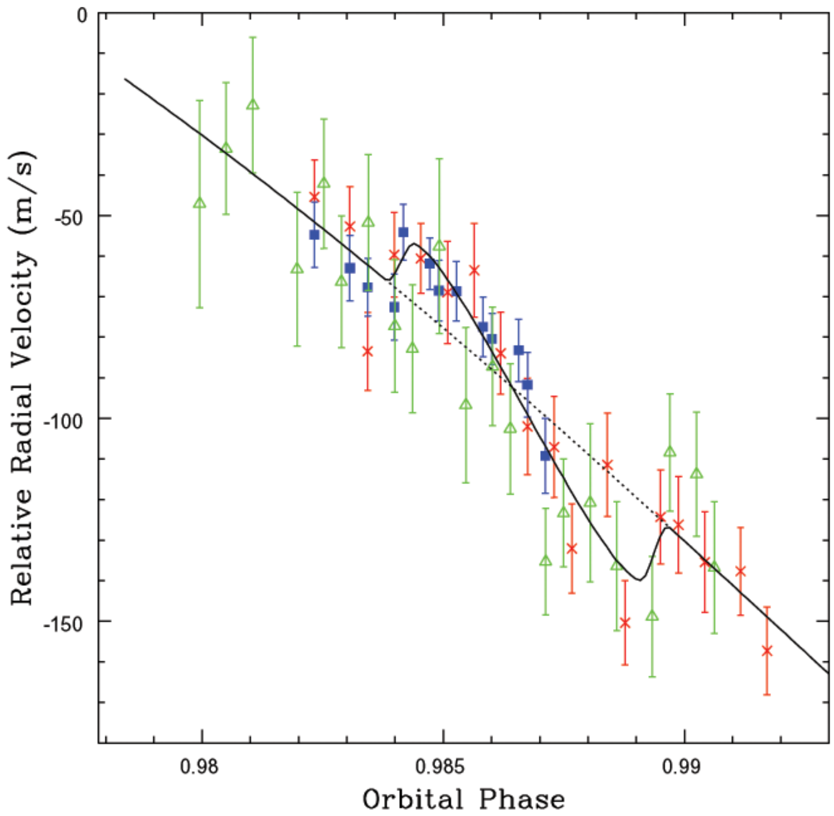

FIG. 1.— The fit of our Rossiter-McLaughlin effect model (solid black line) to the observational data sets. The HJST cs23 data are shown as the (red) Xs, the HET HRS data are (blue) solid squares, and the OAO/HIDES data are (green) open triangles. The dashed black line is the orbital velocity of the star in the absence of any Rossiter-McLaughlin velocity perturbation.

Hebrard et al. 2008

XO-3-b

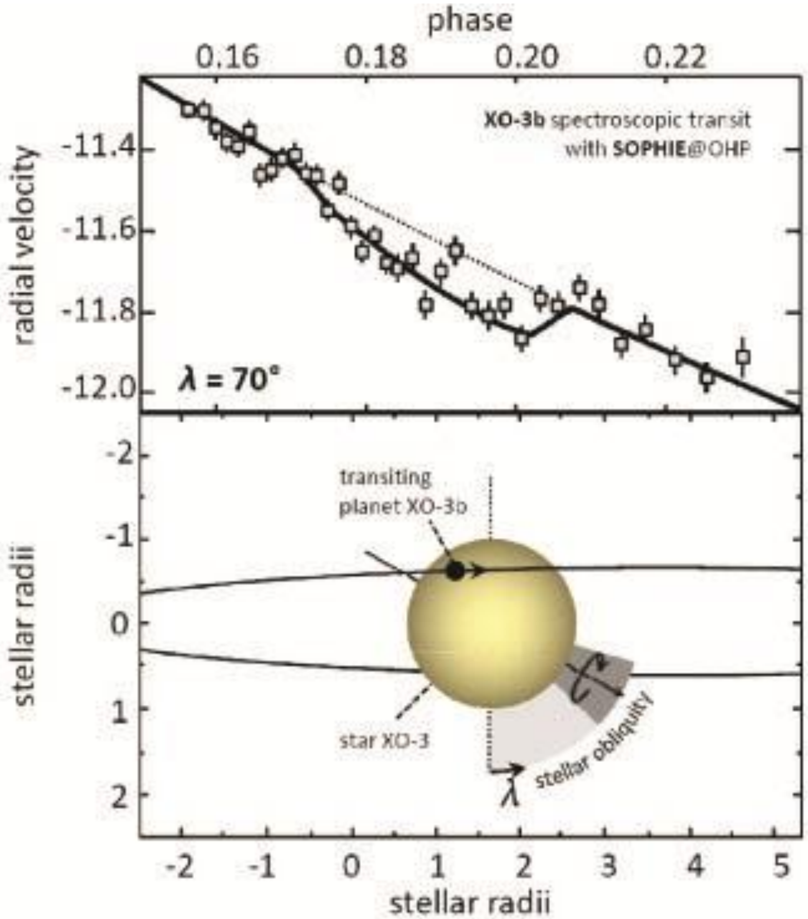

Fig. 2. *Top:* Rossiter-McLaughlin effect models with $\lambda = 70°$. The squares are the SOPHIE radial-velocity measurements of XO-3 with 1-σ error bars as a function of the orbital phase. The solid and dotted lines are the Keplerian fits with and without Rossiter-McLaughlin effect. *Bottom:* Schematic view of the XO-3 system with nearly transverse transit, as seen from the Earth. The stellar spin axis is shown, as well as the planet orbit and the λ misalignment angle (or stellar obliquity). The range $\lambda = 70° \pm 15°$ which is favored by our observations is shown.

λ = 70 degrees

Winn et al. (2009) recent R-M measurements for X0-3

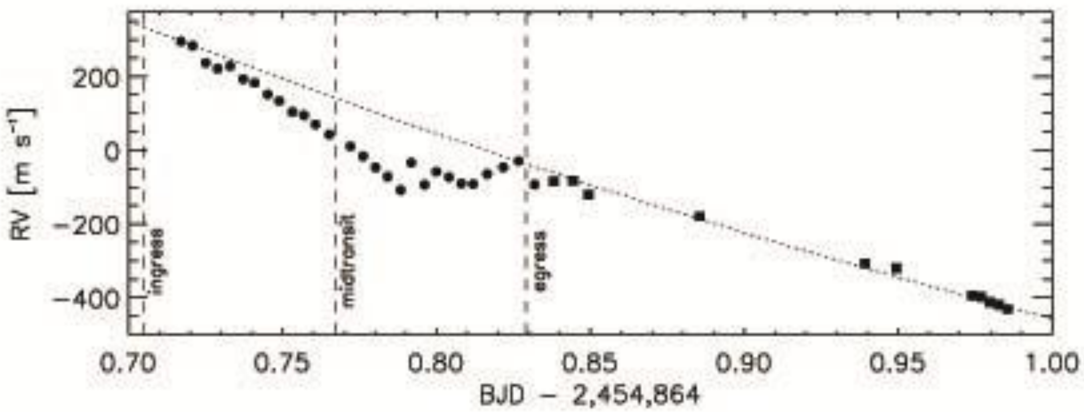

Fig. 1.— **Apparent radial-velocity variation of XO-3 during the 2009 Feb. 2 transit,** based on observations with Keck/HIRES. The internal measurement errors are smaller than the symbol sizes. Dashed lines indicate the photometrically determined times of ingress, midtransit, and egress. The dotted line is the model of the orbital RV variation described in § 3.2.

λ = 37 degrees

Fabricky & Winn, 2009, ApJ, 696, 1230

Table 1
Summary of RM Measurements

Exoplanet	Projected Spin–Orbit Angle λ (deg)	References
HD 189733b	-1.4 ± 1.1	1
HD 209458b	0.1 ± 2.4	2, 3, 4, 5, 6*
HAT-P-1b	3.7 ± 2.1	7
CoRoT-Exo-2b	7.2 ± 4.5	8
HD 149026b	1.9 ± 6.1	9, 6*
HD 17156b	9.4 ± 9.3	10, 11*
TrES-2b	-9.0 ± 12.0	12
HAT-P-2b	1.2 ± 13.4	13*, 14
XO-3b	70.0 ± 15.0	15
WASP-14b	-14.0 ± 17.0	16
TrES-1b	30.0 ± 21.0	17

References: (1) Winn et al. (2006); (2) Queloz et al. (2000); (3) Bundy & Marcy (2000); (4) Wittenmyer et al. (2005); (5) Winn et al. (2005); (6) J. N. Winn & J. A. Johnson (2009, in preparation); (7) Johnson et al. (2008); (8) Bouchy et al. (2008); (9) Wolf et al. (2007); (10) Narita et al. (2008); (11) Cochran et al. (2008); (12) Winn et al. (2008); (13) Winn et al. (2007b); (14) Loeillet et al. (2008); (15) Hebrard et al. (2008); (16) Joshi et al. (2009); (17) Narita et al. (2007). Where multiple references are given, the quoted result is taken from the starred reference.

HAT-P7

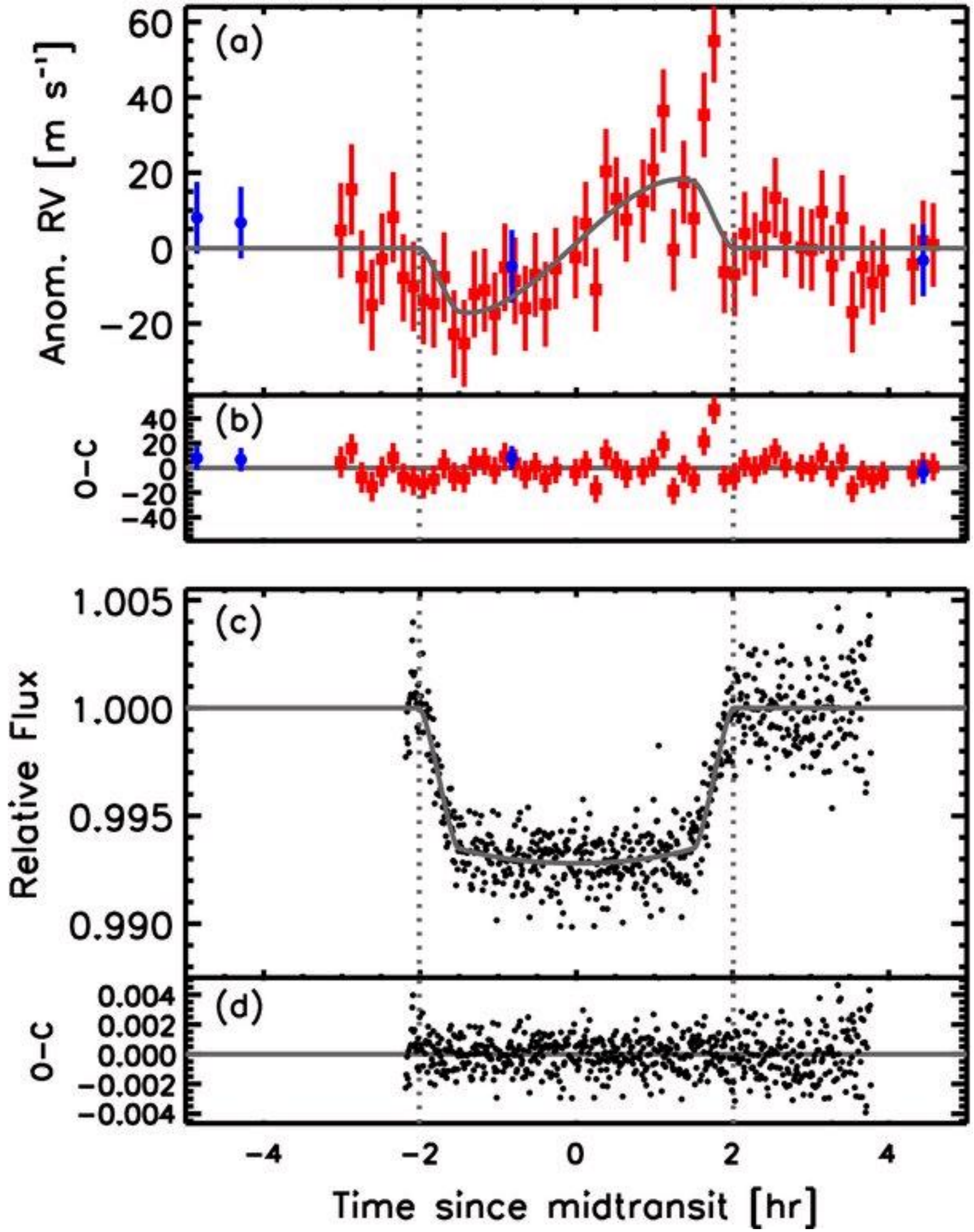

λ = 182 deg!

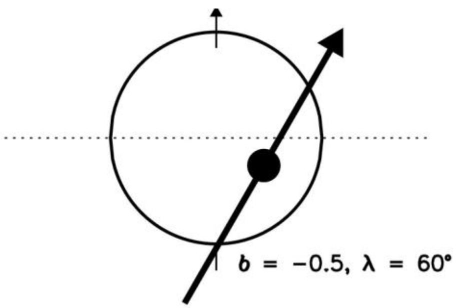

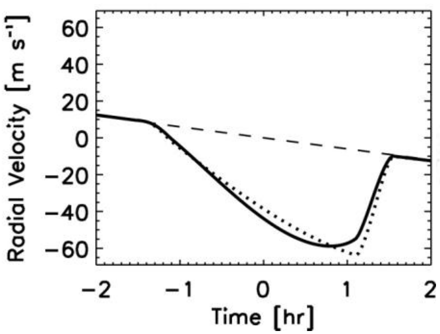

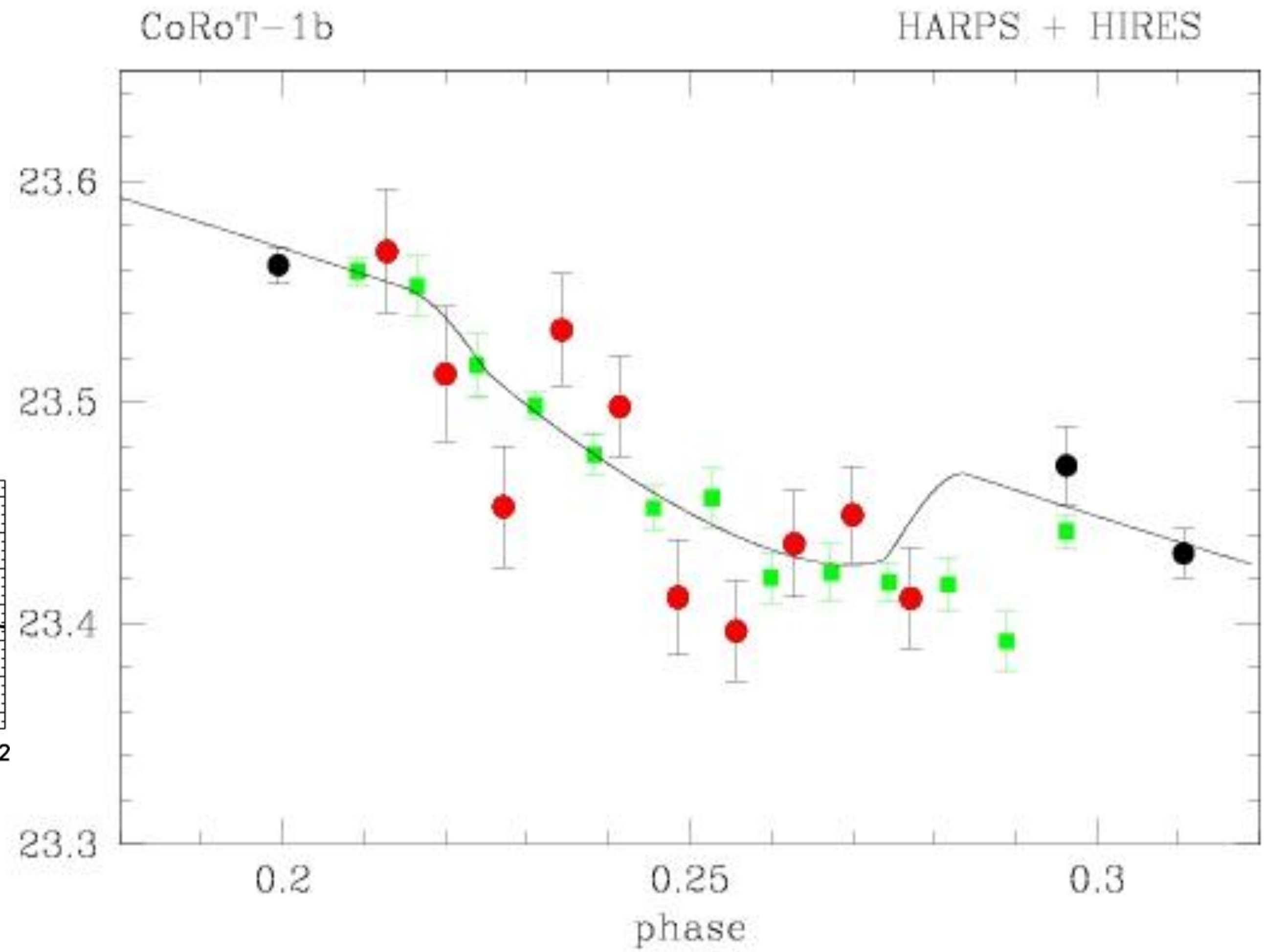

HIRES data: M. Endl HARPS data : F. Bouchy   Model fit: F. Pont

Lambda ~ 80 deg!

Summary of R-M measurements:

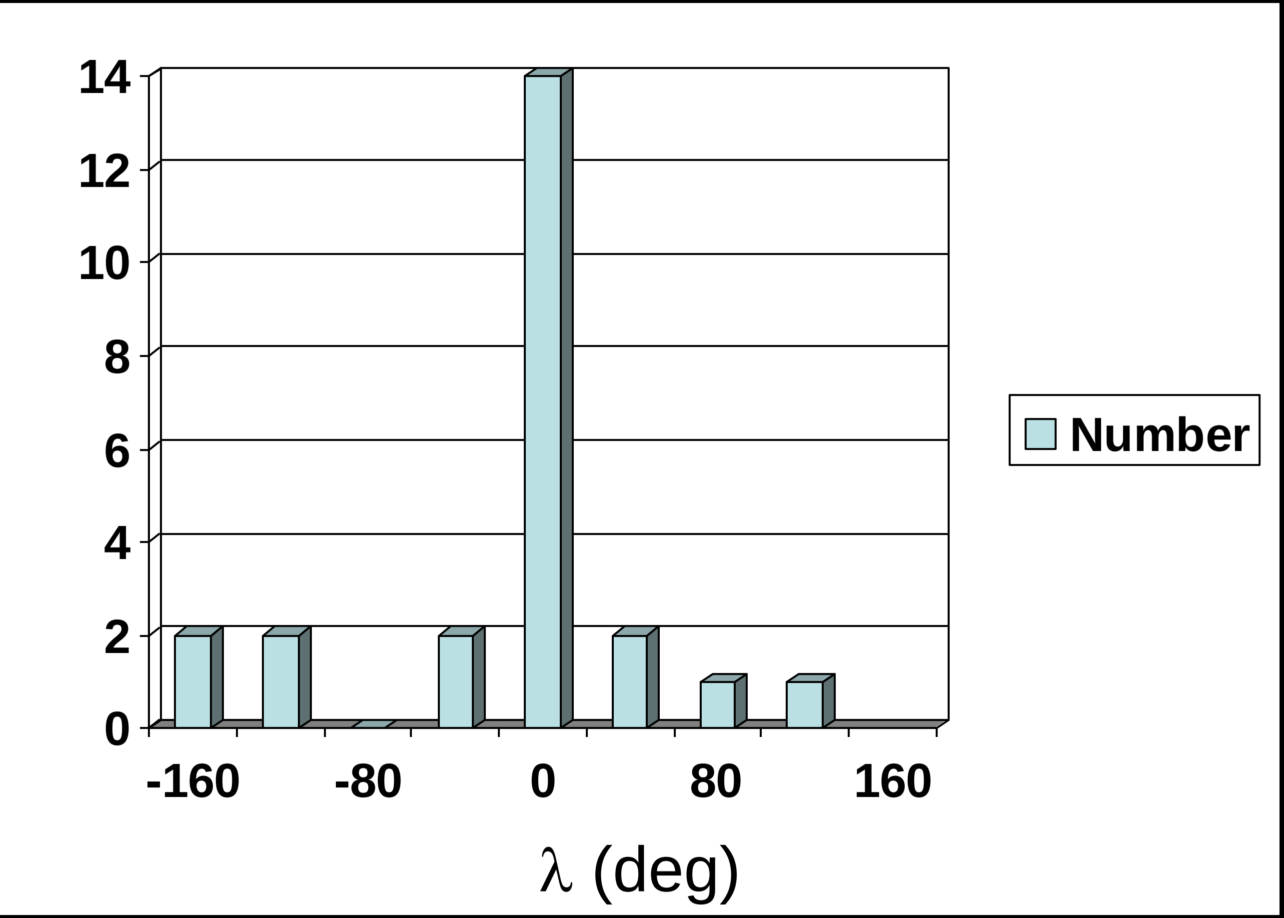

40% of Short Period Exoplanets show significant misalignments

20% of Short Period Exoplanets are even in retrograde orbits

What are the implications? Very violent past, probably due to gravitational scattering of 2 (or more) gas giant planets!